European Commission

nuclear science and technology

Engineered Barrier Emplacement Experiment in Opalinus Clay for the Disposal of Radioactive Waste in Underground Repositories

EB

J-C. Mayor[1], J-L. García-Siñeriz[2], E. Alonso[3], H-J. Alheid[4], P. Blümling[5]

[1] ENRESA, Spain; [2] AITEMIN, Spain; [3] CIMNE, Spain; [4] BGR, Germany; [5] NAGRA, Switzerland

Contract N° FIKW-CT-2000-00017

Final report

Work performed as part of the European Atomic Energy Community's R&T Specific Programme "Nuclear Energy, Key Action: Nuclear Fission Safety 1998-2002"
Area: Safety of the Fuel Cycle

Directorate-General for Reseach
2005 Euratom EUR 21920

ACKNOWLEDGEMENTS

The work has been performed by ENRESA, AITEMIN, BGR, CIMNE and NAGRA with financial support by the European Commission and by the Swiss Federal Office for Education and Science.

The important scientific and technical contributions have been provided by a number of researchers and engineers representing these organizations at the large number of meetings held and in the daily work in the Mont Terri Underground laboratory and at the participants' facilities.

Special thanks are due to the European Commission officer Christophe Davies for his engagement and support of the project in all its phases.

EXECUTIVE SUMMARY

The EB experiment was a full-scale test for the demonstration, in a horizontal drift, of an emplacement technique of the clay barrier, using a granular bentonite material in the upper part of this barrier and bentonite blocks at the bottom. The test has been carried out in a 6 m long section of a niche excavated in Opalinus Clay of the Mont Terri underground laboratory. The experimental layout is shown in the following figure.

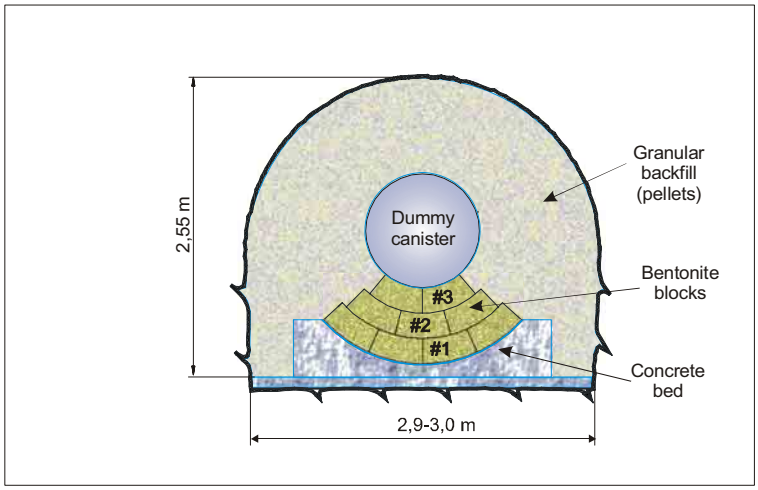

EB experimental layout

A steel dummy canister, with the same dimensions and weight as the real reference canisters, was placed on top of a bed of highly compacted bentonite blocks (in turn lying on a concrete bed), and the rest of the clay barrier volume was backfilled with a Granular Bentonite Material (GBM), made of very highly compacted pellets of different sizes. Hydromechanical instrumentation and an artificial hydration system (to accelerate the saturation of the clay barrier) were installed, and the test section sealed with a concrete plug. The evolution of the hydromechanical parameters along the hydration, both in the barrier and in the clayey rock formation, have been monitored during about 1,5 years, and modelled using the CODE-BRIGHT code.

More specific objectives of the project were the following:

- Definition of the GBM (composition and grain size distribution) and demonstration of its manufacturing at semi-industrial scale.
- Characterization of the hydromechanical properties of the GBM.
- Design and demonstration of the GBM emplacement technique.
- Quality assessment: achieved dry density of the emplaced GBM part of the barrier.
- Characterization and evolution of the Excavation Disturbed Zone (EDZ) of the Opalinus Clay.
- Monitoring of the hydromechanical behaviour of the clay barrier and the rock during the hydration process.
- Development of new constitutive laws of the GBM for the modelling of the test, adjusted with the experimental data.

For the GBM definition, former test results from NAGRA and others were discussed with experts, and new specific trials performed. As a result, a bi-modal pellets mixture, employing two grain size fractions subsequently combined in a second mixing event, was shown to produce high density pellets (greater than 2,10 g/cm^3) and good packing of the mixture. A Spanish bentonite (Serrata de Níjar, Almería) was used for the final production of the GBM. The bulk material was dried and milled to obtain a bentonite powder with water content equal to 3,3%. Then, in a German commercial plant (Rettenmaier) with an automated process (pre-compaction; briquetting; crushing; screening; and mixing) the final GBM was produced. About 47 tonnes were delivered to the Mont Terri site in 63 tightly sealed big bags. When the GBM was actually emplaced in the test section, representative samples were analyzed. The obtained average water content was 4,2%; and the grain size distribution could be represented by the following average values: D_{95} = 10 mm; D_{50} = 6,3 mm; and D_{10} = 0,25 mm.

On the other hand, pellet mixtures with grain size distributions similar to the one of the emplaced GBM where characterized (hydraulic and mechanical tests) in the UPC laboratory (Spain). Due to the double structure of the pellet mixtures (micropores of the pellets and macropores of the mixtures), some novel testing techniques and interpretation procedures had to be developed. Different constitutive responses were observed depending on the wetting rate and on the water transfer type (liquid or vapour). The double structure model seems to be an appropriate framework to better interpret the behaviour of pellet mixtures; which behave as a high-permeability granular material during the first part of a liquid water injection (and even collapse deformations may occur depending on the stress level), but as the pellets start to swell, filling the macropores of the mixture, the permeability decreases substantially. Also, specific and relevant results obtained with the laboratory program are the following:

- It can be estimated that, if the dry density of a GBM is about 1,35 g/cm^3, its saturated hydraulic conductivity is lower than 5×10^{-12} m/s.

- For the same dry density the swelling pressure is ≈ 1,3 MPa.

To emplace the GBM, three types of equipment were first evaluated: a conveyor, an auger and a pneumatic machine. Rowa Engineering designed and manufactured the conveyor and the auger, taking into account the actual work constraints of the EB niche. The evaluated pneumatic equipment was an Aliva 260 Gunnit machine. Emplacement trials were done by Gasser (Lungern) using a full-scale wooden model of the upper part of the actual EB test section. Better results (dry density of the emplaced GBM slightly higher than 1,4 g/cm^3, and no problems with dust) were obtained with the auger. Then, this equipment was selected for the EB experiment.

The 15 m long EB niche (9 m of service area and the 6 m long test section) was excavated in April to June 2001. A road header was used for the test section, to obtain a smooth surface (profile tolerance of ±5 cm). Following, “in situ” geophysical and hydraulic measurements were performed, to characterize the EDZ. From these field surveys, it was concluded that the EDZ reaches a depth of about 0,7 m in the roof of the test section, while at the sidewalls only extends to 0,1 m depth. Also, prior to the GBM emplacement, the rest of the instrumentation to monitor the rock and barrier behaviour during the hydration (16 hygrometers, 20 piezometers, 8 pressure cells, 7 extensometers, seismic sensors and electrode chains); the concrete bed; the bentonite blocks bed (3 layers); and the artificial hydration system (tubing and geotextile mats) were installed. The pre-conditions of the GBM emplacement are shown on the following figure.

Pre-conditions of the GBM emplacement

The GBM emplacement was done with the selected auger in four days (April 2002). The total mass emplaced was 40,2 t in an estimated volume of about 28,4 m^3. As the average water content of the GBM was 4,2%, the obtained dry density of the emplaced material is 1,36 g/cm^3. Quality assurance consisted of carefully determining the weight and water content of the material. A value of the dry density = 1,36 g/cm^3 is lower than the one achieved in the previous model trials (≈ 1,40 g/cm^3), due to the drawback of the presence of the artificial hydration tubing in the test section, which restricted the movements and good working conditions of the auger. It is deemed that, in this experiment, the previous model trials results better demonstrate the achievable dry density of a GBM in a real setting.

After sealing the test section with a concrete plug, the artificial hydration of the clay barrier began in May 2002. Until the end of October 2003 (period of 18 months) in total about 15,2 m^3 of water have been injected. It should be pointed out that in the test section the estimated total air volume (before the start of the water injection) was lower, about 12,5 m^3. A possible explanation for this discrepancy is that some water might be flowing through the rock mass and the concrete plug; although it also can occur that the density of the interstitial water of the bentonite is greater than one. In any case, it can be deducted that, in October 2003, the clay barrier was almost or fully saturated, at least in most of its volume.

At the end of October 2003, recorded total pressures varied between about 1,0 and 1,7 MPa (the highest value corresponds to a sensor installed in the bentonite blocks bed). All the hygrometers placed inside the rock reached full saturation. Also, all the hygrometers (except one) installed in the clay barrier showed full saturation. Fourteen of the twenty piezometers were registering supratmospheric rock porewater pressures, with a maximum of about 1,2 MPa (absolute) in one piezometer located at a depth of 3 m. The other six (located at depths between 0,3 and 1,5 m) were recording values approximately equal to 0,1 MPa. Information provided by the extensometers has shown that the displacements of the rock around the test section have been very small (less than 2 mm). On the other hand, the canister has had greater movements, with a maximum displacement (relative to the rock sidewalls) of about 14 mm.

Hydraulic testing during the experiment period has shown that the rock hydraulic conductivity, in a ring about 80 cm thick around the test section, generally has decreased by two orders of magnitude. The geophysical measurements also have indicated the favourable EDZ evolution during the saturation. With the overall information available, it has been concluded that the EDZ parameters after saturation tend to be the same as those of the intact rock. On the other hand, geophysical measurements carried out in the clay barrier mass indicate that non-fully homogeneous conditions do exist in the barrier, and that probably some spots are not fully saturated.

Two-dimensional modelling of the experiment has been done using the CODE-BRIGHT code. For the rock, the model is able to integrate the elastic degradation along loading and drying paths, brittle behaviour and permeability increase due to damage. In the case of the bentonite blocks, the parameter values used were taken from the FEBEX data. The ones adopted for the GBM were based on the information obtained in the specific laboratory program performed by the UPC, and taking into account the GBM double structure (macro and micropores).

If compared with the monitoring data, the modelling results provide a good estimation of the initial EDZ extent. Also, a reasonably good agreement is found for suction evolution and swelling pressure development. However, monitoring data indicate a heterogeneous behaviour of the clay barrier, which could not be reproduced by the model.

The following main conclusions can be drawn from the EB experiment results:

- Fully automated production of a Granular Bentonite Material (GBM) is possible and large quantities can be produced in due time in the required quality. Only minor modifications of existing production lines in industry for other applications were necessary to achieve this result.

- The use of GBM is a viable option to construct the clay barrier. The methodology developed in the project could be applied in future experiments, although some improvements could be made in order to further increase the dry density of the emplaced GBM.

- Geoelectric and seismic measurements have proven to be a good complement of the hydraulic testing methodology of the EDZ evolution during saturation. The investigations on the time dependent evolution of the EDZ strongly support the hypothesis of EDZ self-sealing in Opalinus Clay, and are thus an excellent completion of the work done in the SELFRAC experiment under contract with the EC, as well.

- The hydromechanical behaviour of the clay barrier and the rock throughout the hydration process is reasonably well understood due to the development of new constitutive laws of the GBM, and their adjustement with the experimental data.

From December 2003 on, the EB experiment is in a latent monitoring phase and close to a full saturation situation, that is the time when the buffer is “fully operative“ and acting on the rock. After this phase, and in order to check the performance of the buffer, the interface buffer/host rock and the influence of the saturated buffer on the EDZ state, dismantling of the test is recommended.

TABLE OF CONTENTS

1 OBJECTIVES AND INNOVATIVE ASPECTS

1.1 Project objectives

The safety of underground permanent repositories relies on a combination of several engineered and geological barriers. The properties of the geological barrier depend on the natural conditions of the rock formation, but the performance of the engineered barriers is a result of their adequate design and execution. In this sense, a reliable technique for the emplacement of the waste canisters and the associated engineered barriers in the underground space is one of the most important parts to guarantee the overall safety.

Some components of the engineered barrier system, such as the fuel package or the canister itself, can be easily controlled during all the phases of construction and assembly, in a factory environment. This control is not so easy in the clay barrier that is being considered in many repository concepts. The construction of this barrier will be carried out in an underground environment, where the access to the barrier space is limited (especially in horizontal type of emplacements), and the correction of potential deviations during the emplacement operation is difficult. The emplacement and backfilling techniques must be, therefore, reliable and easy to control.

One of the options in horizontal drifts is to perform the backfill operation (or at least a part of it) using bentonite pellets. This has in principle many advantages in terms of easier handling and emplacement when compared to the use of large Mennonite blocks, and makes also easier an automated or teleoperated backfill operation. The problem of this emplacement technique is that the final values of the key parameters of the barrier (dry density, permeability, ...) have yet to be demonstrated, at least in the horizontal type of emplacements, where the filling of voids and gaps is more difficult than in a vertical one. The values of the mentioned parameters depend on the initial characteristics of the backfill material, the emplacement technique used, and the Hydro-Mechanical interaction between the backfill and the surrounding rock, which in turn depends on the disturbance caused in the rock during the excavation of the drift.

The “EB Experiment” aims to the “in situ” demonstration of an emplacement technique in horizontal drifts in consolidated clay formations, using pellets as backfill material in the upper part of the clay barrier, and bentonite blocks at the bottom. A full-scale test has been carried out in a drift specially excavated in the Opalinus Clay formation at the Mont Terri underground laboratory. A dummy canister, with the same dimensions and weight as the reference canister, was placed on top of a bed of bentonite blocks, the upper part of the drift being backfilled with a material made of bentonite pellets. The drift was sealed with a concrete plug, and the evolution of the different Hydro-Mechanical (H-M) parameters, both in the barrier and the rock (specially in the EDZ), was monitored for a period of about 1,5 years. Due to the short amount of free water available in this formation, an artificial hydration system was installed to accelerate the hydration process in the backfill. The system was modelled from the H-M point of view, and the data obtained from the test were used to calibrate the model and assess the values of the key parameters of the clay barrier. The basic objectives of the project may be summarised as follows:

- Definition of backfill material (composition, grain size distribution, ..). Demonstration of the manufacturing process at semi-industrial scale.
- Characterisation of the Hydro-Mechanical properties of the backfill material.
- Design and demonstration of the emplacement and backfilling technique.
- Quality Assessment of the clay barrier in terms of the achieved geomechanical parameters (homogeneity, dry density, voids distribution, ...) after emplacement.

- Characterisation of the Excavation Disturbed Zone (EDZ) in the Opalinus Clay, and determination of its influence in the overall performance of the system.
- Investigation of the evolution of the H-M parameters in the clay barrier and the EDZ as a function of the progress of the hydration process.
- Development of a H-M model of the complete system, adjusted with the data resulting from the experiment.

1.2 Innovative aspects

Repository concepts in horizontal drifts have a number of pro and cons in relation with vertical disposal concepts. One of the disadvantages is that the emplacement operation is more complex, this making more difficult the QA aspects of such operation. The current repository concepts in horizontal drifts normally consider a clay barrier that is only made of compacted bentonite blocks, and a significant step forward in the demonstration of the feasibility of this concept has been made in projects like FEBEX. However, the experience gained in this project has also shown that there are a number of technological aspects that may become critical in the real emplacement operation, as for instance the alignment of the steel liner with the drift axis, and the influence of irregularities in the drift rock surface [1]. These aspects could be in principle handled with existing technology, but in any case they introduce additional difficulties in the emplacement operation of a repository of this type, making necessary the use of complex and sophisticated emplacement equipment.

The emplacement layout of this project represents an important innovation for repositories in horizontal drifts. Filling the upper part of the gap between the canister and the rock with a pellets-based type of material makes much simpler the emplacement operation, eliminating some of the most critical aspects of such operation. Main advantages would be:

- The steel liner would not be any more necessary, as the canister can be easily placed vertically on top of the lower bed of bentonite blocks. This reduces considerably the criticality of alignment, and makes easier the QA aspects of the operation.
- The backfill operation can be more easily automated or robotized.
- The air gap between the canister and the liner is eliminated, and this produces a better contact between the canister and the backfill from the very beginning, improving the heat transfer to the rock formation.
- The upper gap between the buffer and the rock surface, that is produced when using bentonite blocks, is also eliminated. This improves again the heat transfer and avoids some of the initial preferential paths for water and gas flow. In the case of rock formations in which an irregular rock surface may be expected from the excavation, as for example consolidated clays, this backfilling technique has advantages in terms of filling voids and gaps. In consequence, more irregular surfaces may be accepted and the excavation and roof support works may be simpler and cheaper.

However, to make possible the use of this backfilling technique, it must be first demonstrated that the values of the key parameters of the buffer achieved by this method, such as dry density, swelling pressure and permeability, fall between the limits considered in the Performance Assessment of the repository concepts, and this is precisely the objective of this project.

Some previous experiences have been carried out in the manufacturing of bentonite pellets and the use of this material for backfill, which have shown the feasibility of the basic aspects concerning such processes. However, the emplacement experiences carried out until now, mainly in the Hades laboratory (Mol,

---

[1] *Final Design and Installation of the FEBEX "In situ" Test at Grimsel. ENRESA Technical Publication No. 12/98.*

Belgium), have been limited to vertical backfills, and have been carried out in a very specific type of rock as it is the Boom clay, which has little in common with more competent formations as consolidated clay or granites. Bentonite pellets have also been used at the Äspö laboratory for backfilling horizontal tunnels (for example in the "Backfill and Plug" Test), but in this case the concept is totally different and the pellets have only been used in small areas of the cross-section, as an auxiliary way of completing the backfill. In all cases, the emplacement of the pellets backfill has been made either manually or using specific emplacement techniques which would not be applicable in a horizontal type of repository.

Therefore, a full scale test was required in a realistic environment, to demonstrate the feasibility of this backfilling technique in a horizontal drift. It is also necessary to check the obtained values in the key parameters, and the homogeneity of such parameters across the entire buffer volume.

On the other hand, no previous experiences existed on emplacement of real size canisters and backfilling of drifts in consolidated clay formations. This implied that a number of problems had to be solved, which increased the innovative aspect of the project:

- The excavation of the drift in the Opalinus Clay for this type of experiment is by itself an important new issue that required a detailed study, as a number of different aspects have to be taken into account: required cross-section and shape, surface roughness, temporary and/or permanent roof support, extension of the EDZ, ...
- The emplacement technique for the pellets backfill had to be conceived and tested. This operation required the transport of the material several meters in horizontal, and a correct and uniform distribution across all the void volume. Methodologies for the Quality Assurance of the backfill operation had also to be developed.
- An artificial hydration system had to be developed to accelerate the progress of saturation process. A system of this size and characteristics had not been yet developed in consolidated clays.
- The role of the EDZ in consolidated clays may be important in the overall performance of the engineered barrier system. Some research works have already been carried out at the Mont Terri laboratory in relation with the EDZ and its self-sealing capacity, but as the characteristics of the EDZ vary a lot depending on the excavation method used and the scale of the void, the results may be quite different in this case. The interaction of the EDZ with the bentonite, and the effects of re-saturation, had not been studied before at this scale.
- The parameters of the pellets-based backfill were not known, and this required a number of laboratory tests to characterise the properties of this material. The heterogeneity of the material also required modifications in the H-M models being currently used.
- The combination of different types of material in the clay buffer (bentonite blocks and pellets backfill) is a new approach that introduced new difficulties in the understanding and modelling of the system performance.

2 EB EXPERIMENT DESIGN

2.1 Location and test layout

The experiment has been carried out in a short gallery excavated for this purpose, identified as "EB niche". It is located at the end of the DI niche and it is parallel to the "new gallery" of the Mont Terri Underground Rock Laboratory, on its shaly facies section (Figure 1). The EB niche is 15 m long. It has a horseshoe section, 2,55 m high and 3 m wide (Figure 2).

The aim was to install a dummy canister, of the same dimensions and weight than the reference canister, on the top of a bentonite blocks bed. The remaining gap between the canister and the rock was backfilled with bentonite pellets (Figure 2). The experimental area was isolated by a concrete plug (Figure 3).

To accelerate the hydration process an artificial system was installed. This system is comprised of a combination of pipes and mats arranged around the canister. To monitor the evolution of the experiment, different sensors and a data acquisition system were installed, including remote access.

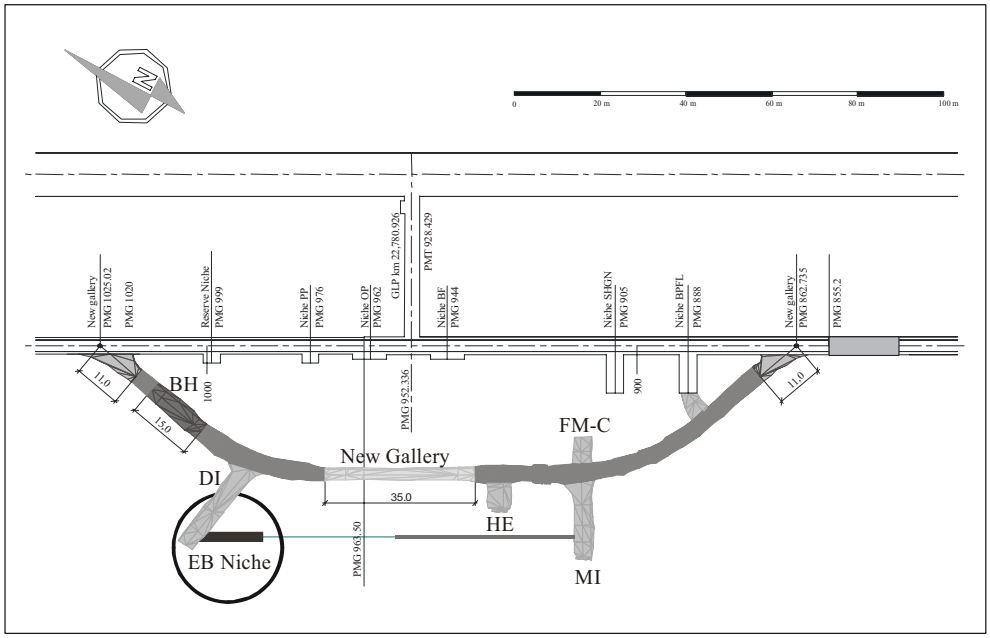

Figure 1: Location of EB Niche in Mont Terri URL

2.2 Concrete bed

It is a mass concrete bed of the same length than the dummy canister and with a circular shape. It does not contain any steel re-enforcement due to geophysical requirements. The circular shape of the concrete bed allows to use bentonite blocks of the FEBEX project.

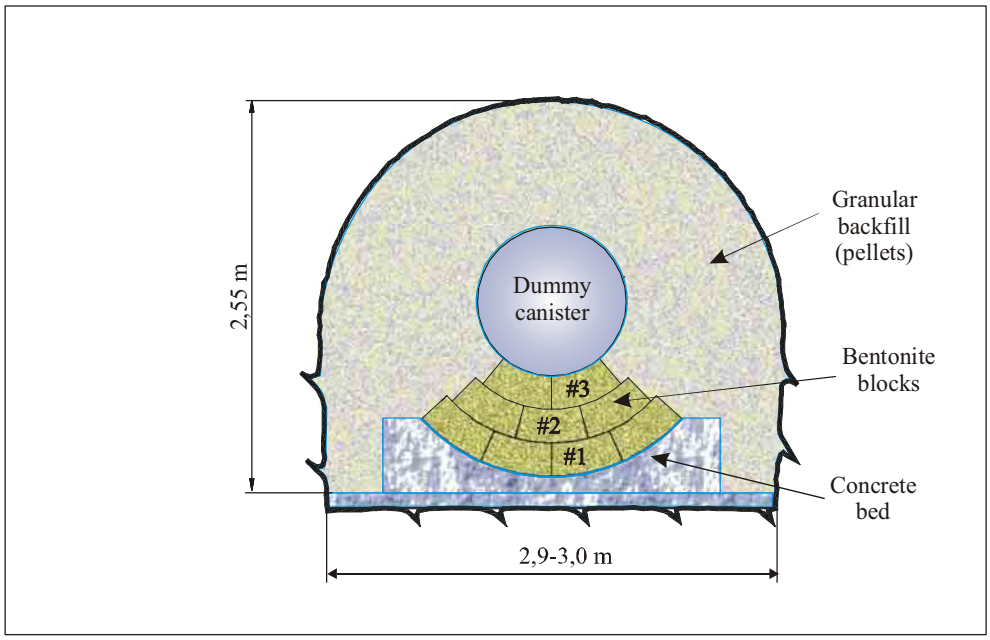

Figure 2: EB experimental layout

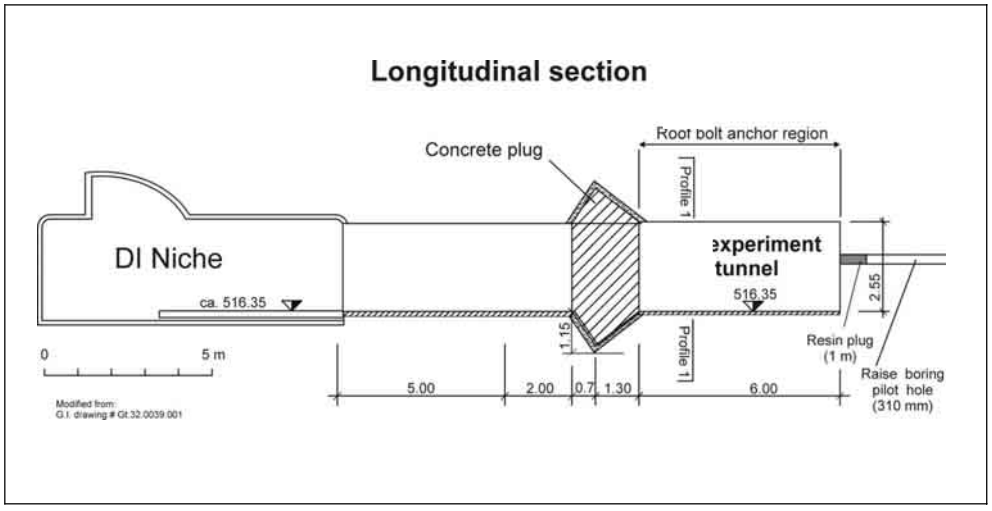

Figure 3: EB niche, longitudinal section

2.3 Bentonite blocks bed

The blocks, coming from the FEBEX project, have a dry density of 1,69 g/cm^3 and the water content was 14,36 %. The dimensions of blocks are given in Table 1 and Figure 4. The bentonite blocks bed is composed by three layers (#1, #2 and #3); see Figure 2 for their position.

Table 1: Characteristics of bentonite blocks

Block type	a (mm)	b (mm)	c (mm)	Thickness (mm)	R (mm)	r (mm)	α (°)	Weight (kg)
#1	$470{,}0^{+2{,}0}_{-5{,}0}$	$380{,}0^{+2{,}0}_{-4{,}0}$	$214{,}0^{+2{,}0}_{-3{,}0}$	$125{,}0^{+2{,}0}_{-2{,}0}$	1,133	919	24°	22,1
#2	$473{,}0^{+2{,}0}_{-5{,}0}$	$361{,}0^{+2{,}0}_{-4{,}0}$	$214{,}0^{+2{,}0}_{-3{,}0}$	$125{,}0^{+2{,}0}_{-2{,}0}$	917	703	30°	21,8
#3	$478{,}0^{+2{,}0}_{-5{,}0}$	$330{,}0^{+2{,}0}_{-4{,}0}$	$214{,}0^{+2{,}0}_{-3{,}0}$	$125{,}0^{+2{,}0}_{-2{,}0}$	701	487	40°	21,3

2.4 Dummy canister

The dummy canister used in the experiment is similar in weight and dimensions to the one in the ENRESA and NAGRA reference concepts, and has a length of 4,54 m and a diameter of 0,97 m. It was made of carbon steel and filled of a barite emulsion, density 2,65 g/m^3, to obtain the needed weight, being the empty weight of 4000 kg and the final weight approximately 11000 kg.

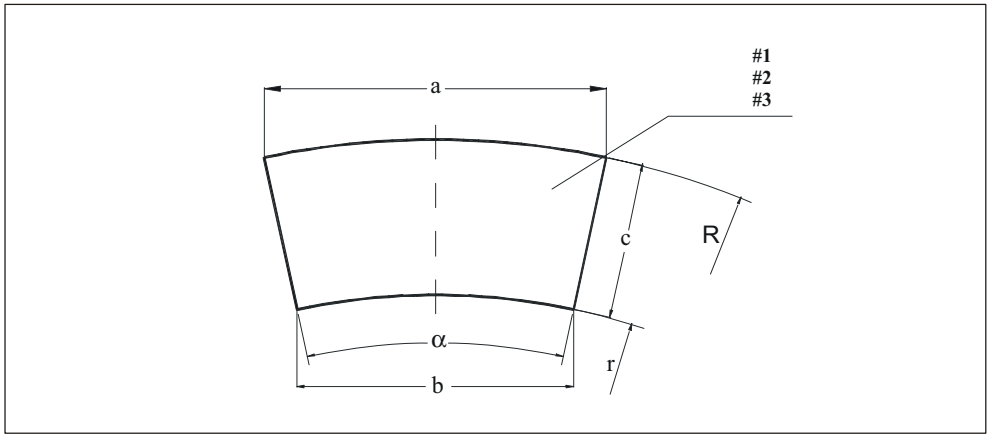

Figure 4: Dimensions of FEBEX bentonite blocks

2.5 Hydration system

The EB hydration system has two separated parts: test and service area.

Test area components of the hydration system include the hydration tubes and geotextile hydration mats. Figure 5 shows the distribution of tubes and hydration mats around the canister and between the bentonite blocks. A water distribution system feeds the hydration tubes and geotextile mats at different levels: floor level, canister level and top level. Figure 5 also includes the elements of support (Kevlar® cables and Nylon® rods).

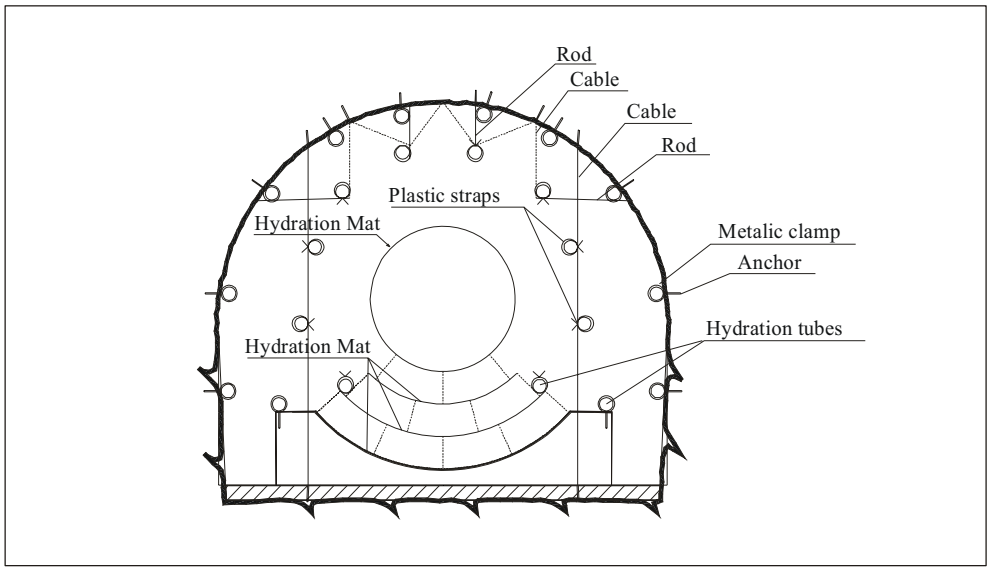

Figure 5: Scheme of Hydration system and support (cross-section). Position of hydration tubes, hydration mats and bentonite blocks

At the service area (Figure 6) a water tank feeds an air operated pump. The water used is synthetic and its composition is chemically equivalent to the Opalinus Clay formation water.

Water flow and pressure are controlled by compressed air supplied by a compressor. The pump injects the water to the three distribution main lines that can be isolated by means of two-way ball valves.

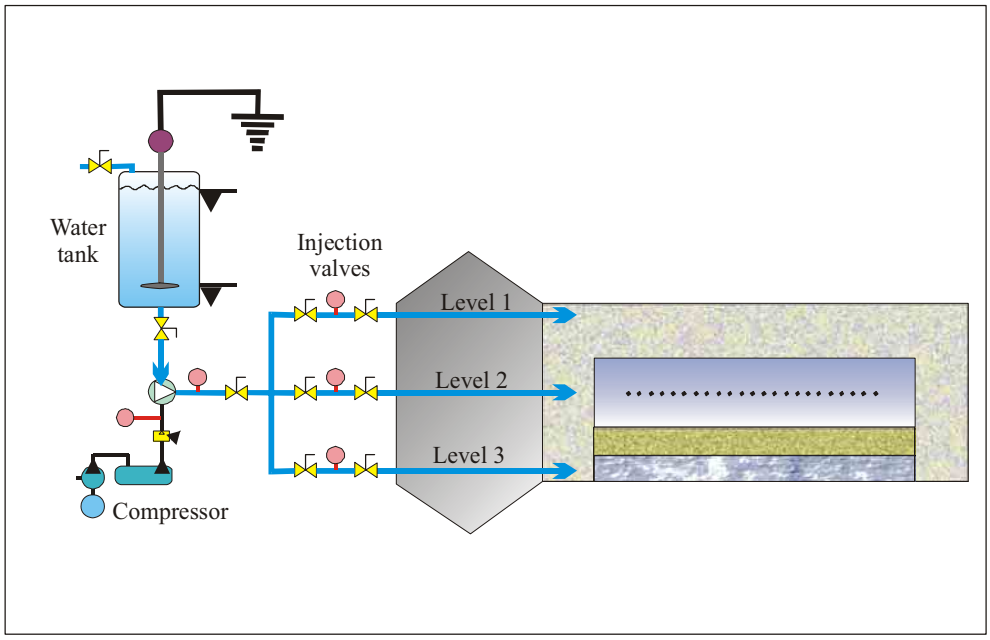

Figure 6: Scheme of the hydration system (general layout)

2.6 Instrumentation

To monitor the relative humidity, temperature, pore and total pressure and displacements, sensors were installed in different sections along the niche. See the position of sections and examples of sensors' positioning in Figure 7 to 10. They are the following:

For measurements in the rock mass:

- 20 Piezometers
- 8 Capacitive humidity sensors
- 3 Extensometers
- Seismic sensors
- Electrode chains

For measurements in the bentonite buffer:

- 8 Total pressure cells
- 4 Extensometers (for canister displacements)
- 8 Capacitive humidity sensors

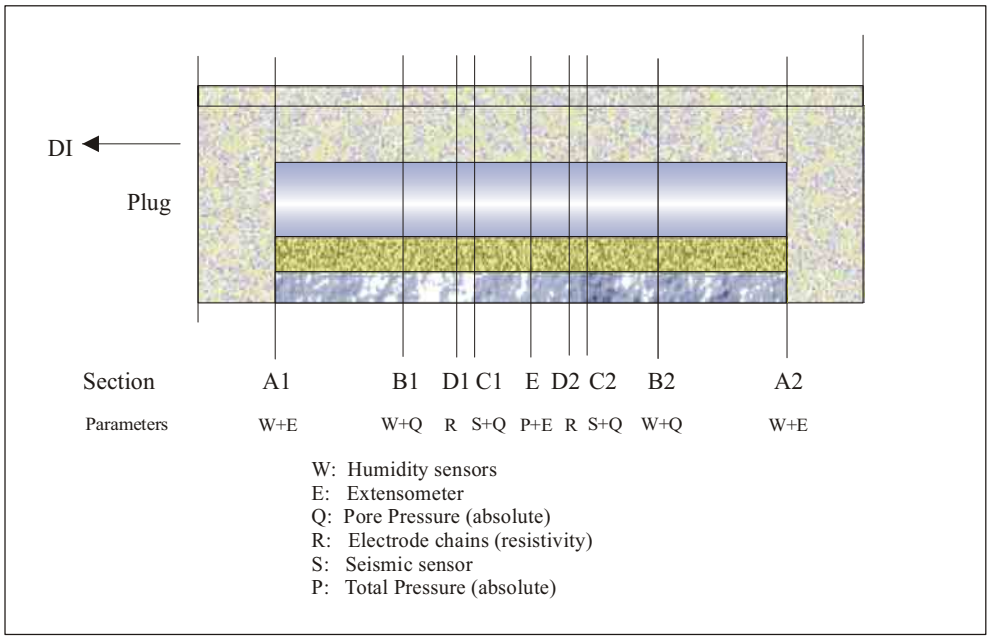

Figure 7: Position of instrumented sections in EB Niche

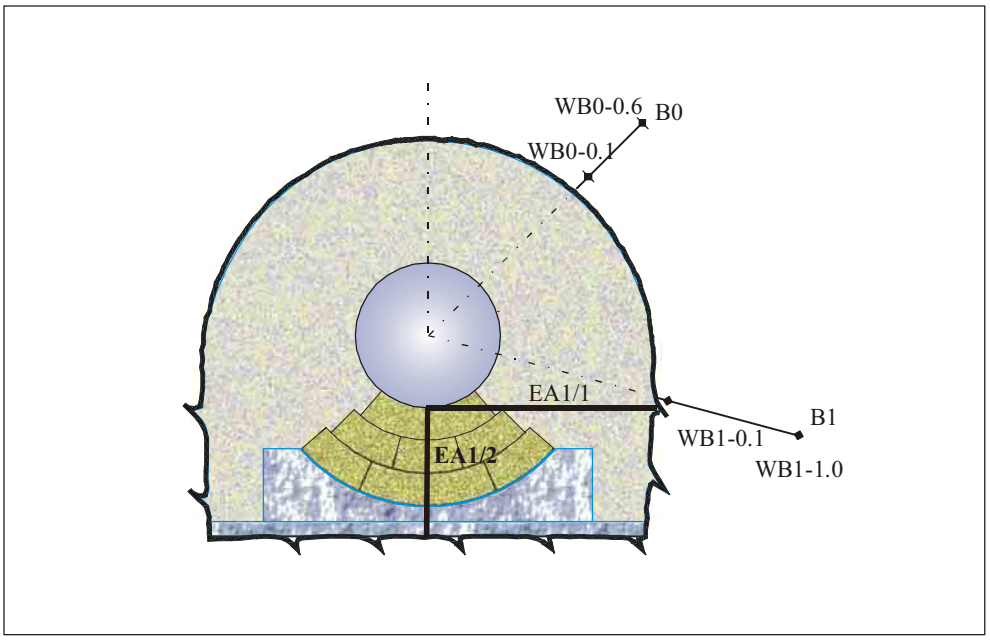

Figure 8: Section A1, rock relative humidity and canister displacement sensors (coding WB0-x, where x indicates depth in m)

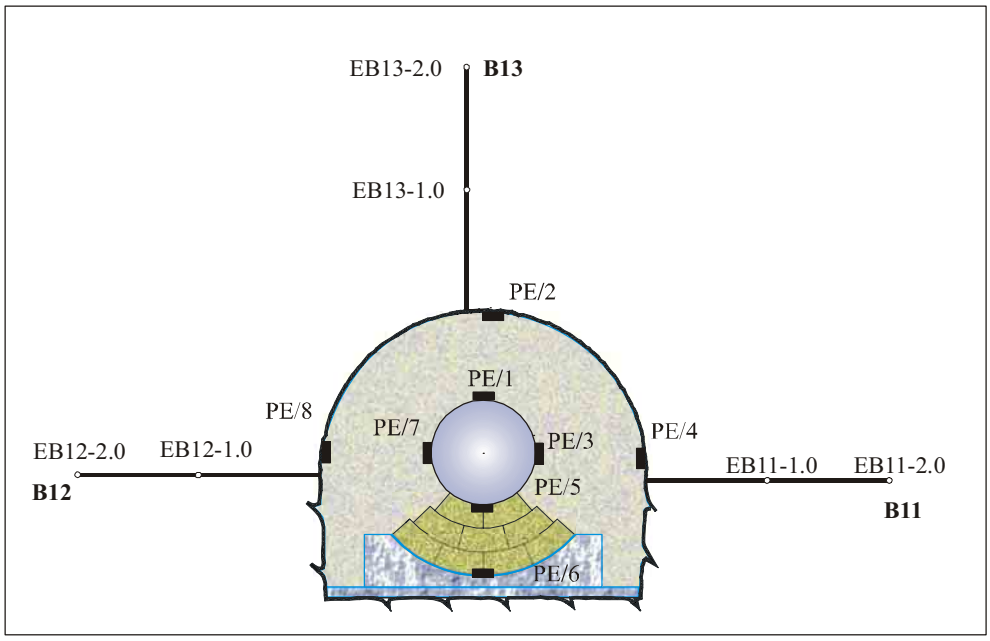

Figure 9: Section E, rock displacement sensors and total pressure cells (coding EB12-x, where x indicates depth in m)

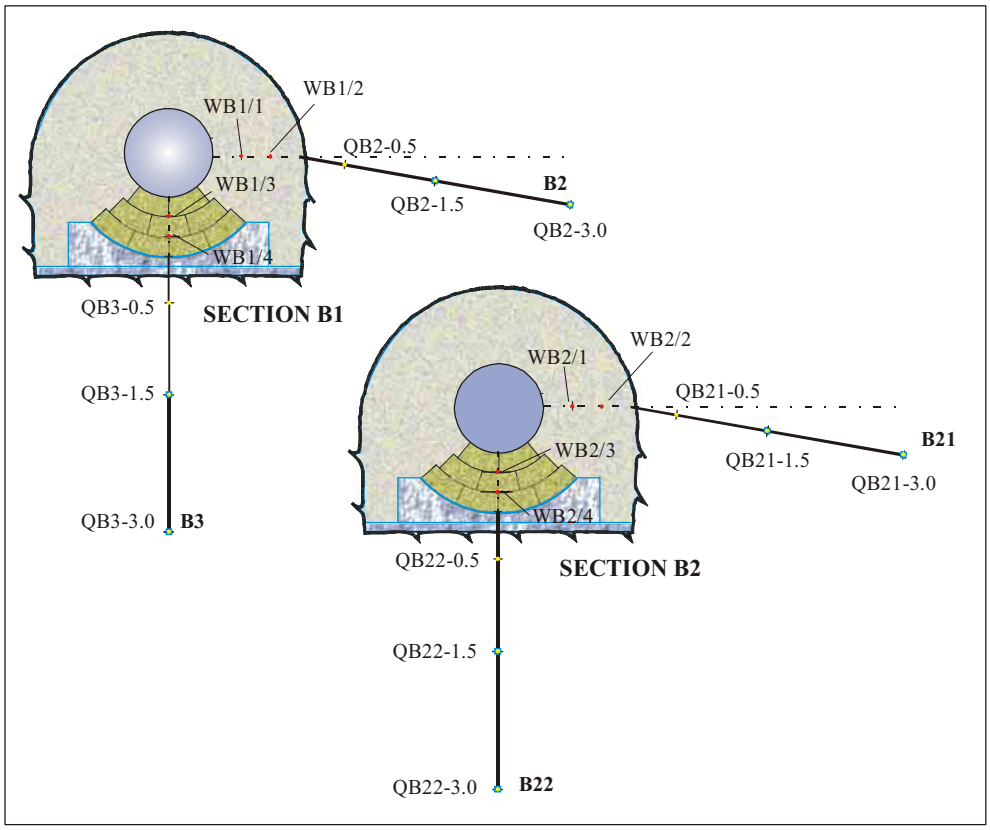

Figure 10: Sections B1 and B2, buffer relative humidity and rock pore pressure sensors (coding QB22-x, where x indicates depth in m)

2.7 Data acquisition and monitoring system

Two independent data acquisition and monitoring systems were installed: one for the geomechanical and hydraulic (HM) parameters, and another one for the EDZ monitoring.

The design of HM monitoring and control system was determined by the requirements of unattended working and remote control. There is a "Local Monitoring System" (LMS) for the monitoring and control of the test and for long time data storage. A "Remote Monitoring System" (RMS) was installed in AITEMIN control office in Madrid. Both systems are linked by modem.

Both systems work in an unattended mode most part of the time and only connect between themselves by means of the communications system for periodic data recovery from RMS and for introducing changes in the monitoring schedule. Automatic data collection from all sensors that work in a continuous mode (pressure, humidity, displacement) started on 30th April 2002 and continued for an indefinite period after the end of the contract with the European Commission.

3 BACKFILL MATERIAL

3.1 Buffer fabrication

The blocks have a dry density of 1,69 g/cm^3 and water content of about 14%. The blocks dimensions are based on the geometry of the FEBEX drift and heater liner. The material is a bentonite from Serrata de Nijar (Almería, Spain). A brief summary of its main characteristics is given in Table 2.

Table 2: FEBEX bentonite characteristics

Smectite content	88 – 96 %
Water content	12,4 – 15 %
Grain size	< 5 mm
Fraction under 74 µm	93 %
Fraction under 2 µm	65 %
Liquid limit	103 %
Specific gravity	2,71
Specific surface	32 m^2/g

For the granular bentonite buffer, the most critical points are the achievement of very high pellets density and an appropriate grain size distribution. Results of former trials and literature data were discussed with experts having extensive experience using these materials. The main concerns were the type and quality of the bentonite and the grain size distribution of the final product after creating first the pellets/briquettes and then milling/breaking/screening/ and finally producing the end product: a Granular Bentonite Material (GBM) of adequate grain size distribution.

Calcigel was selected for the trials and pilot testing of the processes to be used for the GBM production. Discussions with experts established that this type of bentonite should sufficiently resemble the Spanish bentonite, particularly with regard to the briquetting behaviour. The bentonite could be delivered with a moisture content of about 6 percent and as a powder with existing processing plants and in-line production facilities.

For the GBM grain size distribution, theoretical approaches and former test results from NAGRA and others were reviewed and discussed. As a first target, a curve for the sizes from 0,5 to 10 mm was defined based on dense packing of spheres. A second grain size distribution still needed to be defined and it was decided to use a binary mixture.

The optimal water content for compaction of a bentonite powder into high density pellets has been determined in bench-scale testing using realistic agglomeration and compaction equipment to be in the range of 4 percent.

Trials to select and then demonstrate production of a granular backfill material were successful. They showed that an existing commercially available process could be used with minor modifications to achieve production of compressed bentonite pellets in the 5 to 15 mm size range with dry densities of about 2,2 g/cm^3 when the water content was in the range from about 5 to 6 percent. The trials used Calcigel, but pilot scale batch testing with the Spanish Serrata bentonite achieved similar results with lower water contents of about 4 percent.

To optimise the process of creating a material that had both good packing and high density characteristics, the specification selected to do this was the Simonis curve. To meet the specification, a bi-modal mixture employing two grain size fractions subsequently combined in a second mixing event was shown to produce even better results than using just a single stage of production. The impact of the second mixing served to further round the materials and produce some additional high-density finer grains.

For the final production materials, Serrata bentonite from an inactive Spanish quarry site was used. About 100 tons of bulk, partially air-dried and screened material were produced. This material was then dried and milled in a three step process to produce a 60 ton batch of fine grade bentonite powder with a water content of 3,3 percent. A commercial plant with an in-line highly automated briquetting process (Figure 11) produced about 32 tons of coarse grained (> 7 mm) and about 19 tons of fine (0,4 to 2 mm) material. Coarse material average pellet density was 2,18 g/cm^3 with a water content of 3,3 percent; the dry density was 2,11 g/cm^3. The fine materials had a pellet density of 2,21 g/cm^3 with a water content of 3,7 percent; the dry density was 2,13 g/cm^3.

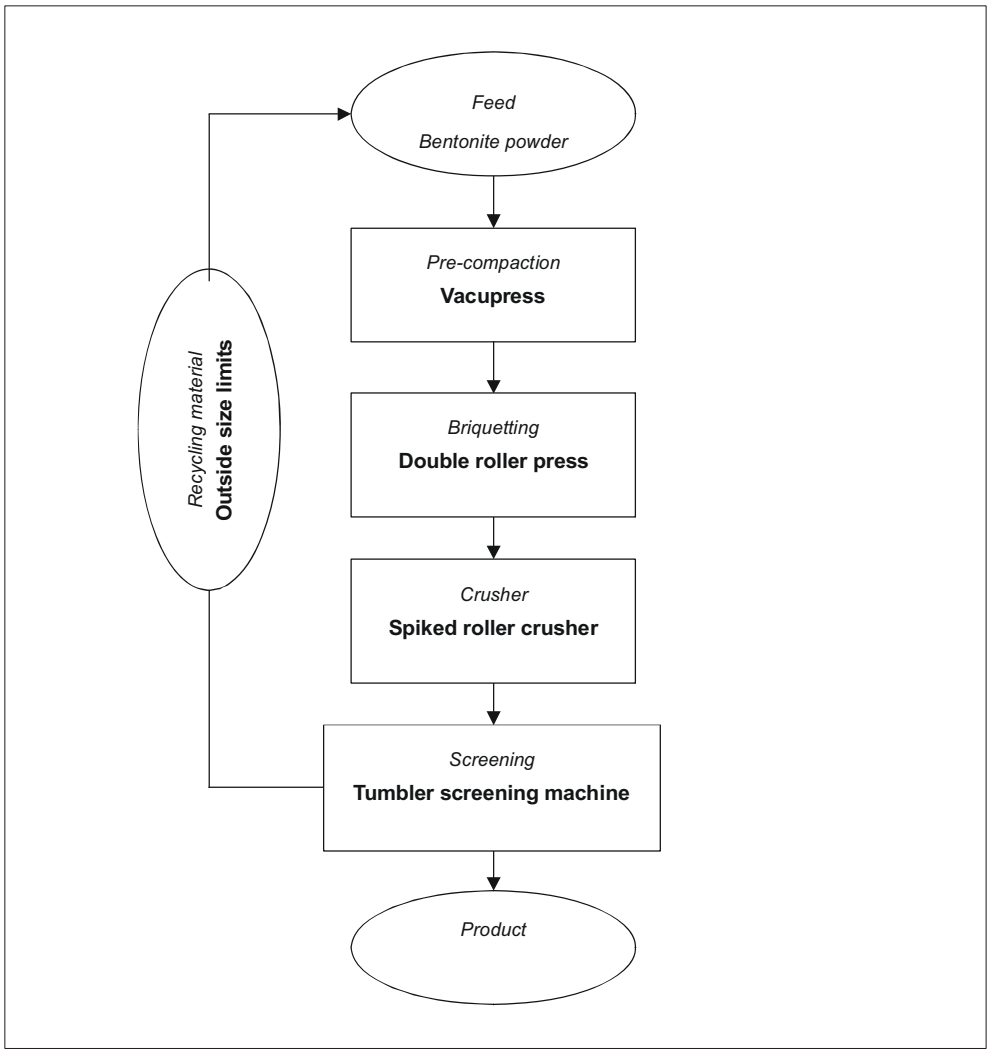

Figure 11: Schematic flow diagram for the processing

Mixing trials using a drum and a cement mixer were done to determine an optimal secondary mixing method.

The material was shipped to the Mont Terri site in tightly sealed and shrink-wrapped big bags with weights averaging about 750 kg.

3.2 Granular Bentonite Material (GBM) emplacement equipment

Three types of equipment were evaluated for the emplacement, namely a conveyor, auger and pneumatic method (Figure 12). NAGRA had conducted borehole filling experiments about a decade earlier and had achieved bulk densities on the order of 1,4 to 1,5 g/cm^3 with the use of a pneumatic method and high density granular backfill materials made from MX-80 bentonite. These experiments were done using smaller volumes of materials due to the boreholes sizes. However, the emplacement using a pneumatic method had involved the use of extensive lengths of tubing during the materials transport.

Figure 12: Emplacement equipment: A) conveyor B) auger C) Gunnite machine

The evaluation of the different methods were done using the following methodology steps:

- Equipment review
- Preliminary design and quotation
- Equipment design, manufacturing, commissioning
- Materials evaluation and production
- Method evaluation – preparation
- Conveyor trial without and with pneumatic completion
- Auger trials without and with pneumatic completion in full and ½ model
- Pneumatic trial in ½ model
- Equipment and method assessment

Rowa Engineering AG (CH) was contracted to design, manufacture and assemble the conveyor and the auger. Both had to work within the constraints of the tunnel setting. At the same time, the materials had to be able to be transported from an access point. For this reason, a multi-purpose transfer wagon was proposed to be used as a supply mechanism for both the conveyor and the auger.

The conveyor is about 7 m long and about 0,75 m wide. It receives the GBM from the transfer wagon as it drops onto the running belt and transmits it to the other end where the material falls off the end of the belt. The belt is cleaned just after the rotation spot at its end so that it return without any residual materials to the start position. The feed rate of the conveyor is controlled by the feed rate from the transfer wagon.

The auger is about 7 m long and the outside casing is about 0,20 m in diameter. The auger screw receives the GBM from the transfer wagon as it drops into the auger's own hopper. The auger moves the material to the end of the outer casing tube where it either falls off freely or it can be pushed out into an existing mass. The feed rate is controlled by the auger turning speed.

A pneumatic shotcrete machine (Aliva 260 Gunnit) was evaluated early in the process. Of the three methods, the pneumatic was believed to potentially change the materials properties the most, so the pneumatic method was left until all other trials had been conducted.

A total of six separate emplacement trials were undertaken at the Gasser Felstechnik Facilities in Lungern (CH). The facility at Gasser was selected because it is underground and has a constant temperature and relatively constant, albeit high humidity environment. Trials began in late August 2001 and the first five were completed within about one month. Due to technical reasons, the sixth and final pneumatic trial was postponed until mid - October 2001.

The essential components of the trials included a wooden model of the upper part of the tunnel and weighing methods for the big bags. The model was designed and built in a modular fashion by Gasser in place (Figure 13 and Figure 14).

Sampling of the materials as they were taken from the big bags were done for most of the trials by ETH, Zürich. They carried out analysis for density and porosity, water content, bulk and emplacement density and grain size distribution. They also assisted in evaluating the distribution of the densities and grain size distributions within the model according to the emplacement method by taking samples as the materials were being offloaded manually. Great care was taken to obtain undisturbed samples during this offloading. Manual sampling using 7 cm diameter by 7 cm high cylinders was done.

The three methods used were compared. The conveyor does not provide suitable opportunities for additional packing or filling of lateral and overhead void spaces so it is not an appropriate technique. The pneumatic method achieved the second best of the three emplacement trial results. However, operationally this method is severely complicated by the fine dust fraction produced. Finally, there is no question that the emplacement results of dry densities between 1,40 and 1,41 g/cm^3 using the auger were better than either of the two other methods evaluated. In addition, the auger method had little problems with fugitive dust.

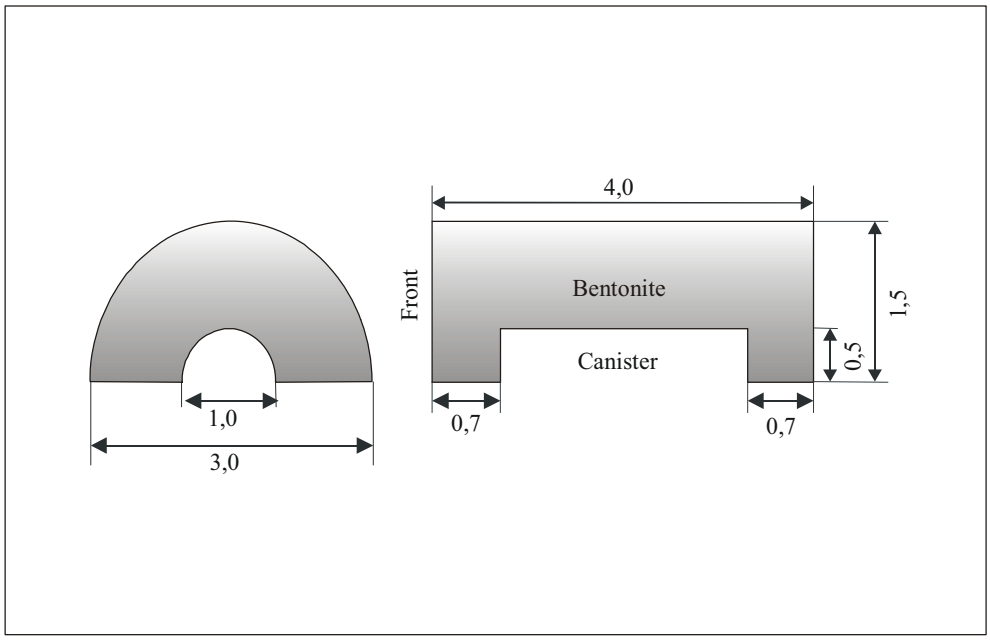

Figure 13: Model layout for the emplacement testing trials (dimensions in m)

Figure 14: Wooden model: measuring heights and dimensions prior to final assembly

3.3 GBM laboratory hydraulic and mechanical characterization

For the laboratory test program (conducted by UPC, Spain) grain size distribution of pellet mixtures were based on the Fuller grading curve. In addition, particles with sizes less than 0,4 mm were disregarded in order to avoid segregation of the finer fraction. Figure 15 shows the idealized "Fuller" packing and the actual grain size distribution used in tests.

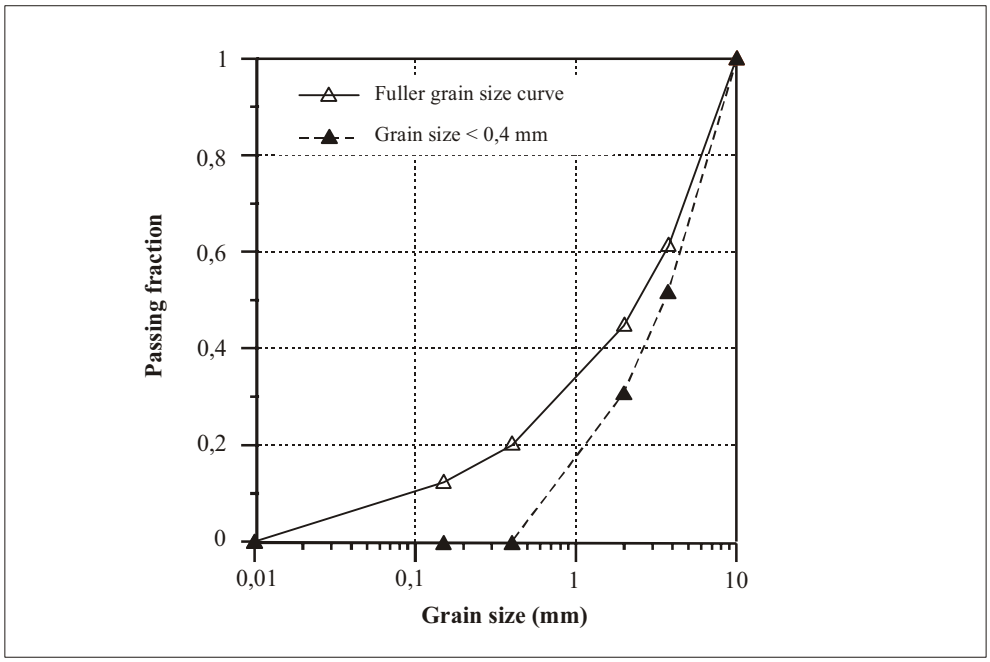

Figure 15: Grain size distribution curve. Mixture with Dmax = 10 mm and Fuller grading curve for the same Dmax

The maximum size (D_{max}) for each mixture was selected considering the sample size of the different cells. D_{max}= 4 mm was used for test series performed on samples 50 mm in diameter and 20 mm high. On the other hand, values of D_{max} = 10 or 15 mm were used for tests performed on samples 50 or 75 mm in diameter and 50 or 100 mm high, respectively. Other grading mixtures were used in special tests like flux tests where a uniform pellet size of 4 mm was adopted.

Pellets mixtures with dry density values varying from 1,05 to 1,9 g/cm^3 were tested; with special emphasis to testing samples having dry density values in the range 1,3 to 1,5 g/cm^3. Results obtained are discussed under two headings: hydraulic and mechanical properties.

3.3.1 Hydraulic properties

Water retention curves

Wetting and drying suction controlled paths were applied on samples and the corresponding water content was measured. Water retention curves for drying paths and dry density values of 1,3, 1,5 and 1,9 g/cm^3 are presented in Figure 16. A modified Van Genuchten expression was fitted to the experimental data.

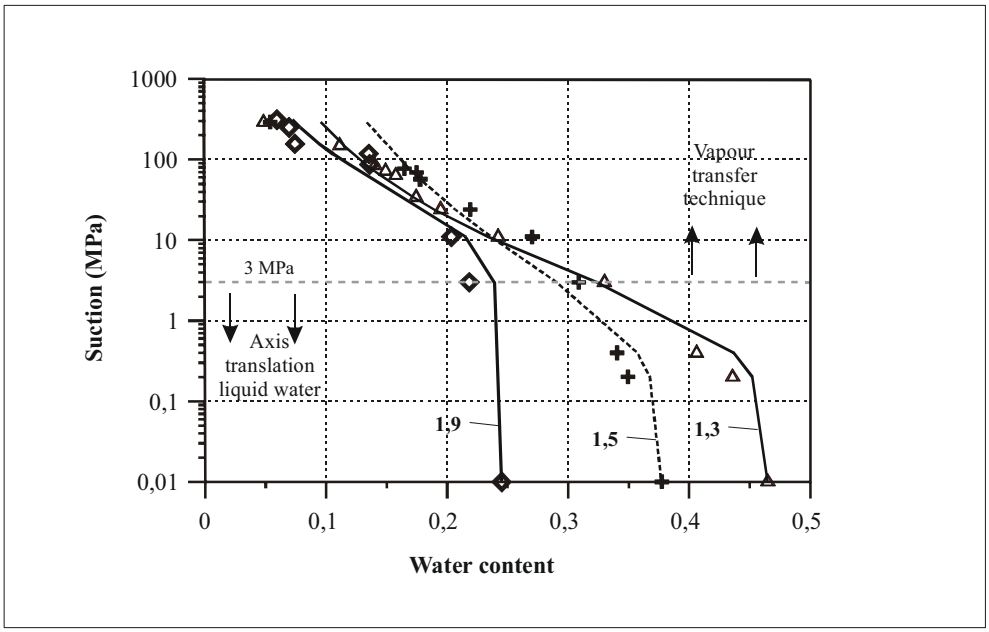

Figure 16: Water retention curves during wetting paths for bentonite pellet mixture with dry densities of 1,3, 1,5 and 1,9 g/cm3

Permeability

Constant gradient permeability tests were performed on samples with dry density values varying from 1,05 to 1,6 g/cm^3. Water flows entering and leaving the specimen were monitored until steady state conditions were approached. At this time the sample was assumed to be saturated and the hydraulic conductivity was calculated. Saturated hydraulic conductivity values obtained during these tests are presented in Figure 17. For comparison purposes FEBEX data are also shown in the figure.

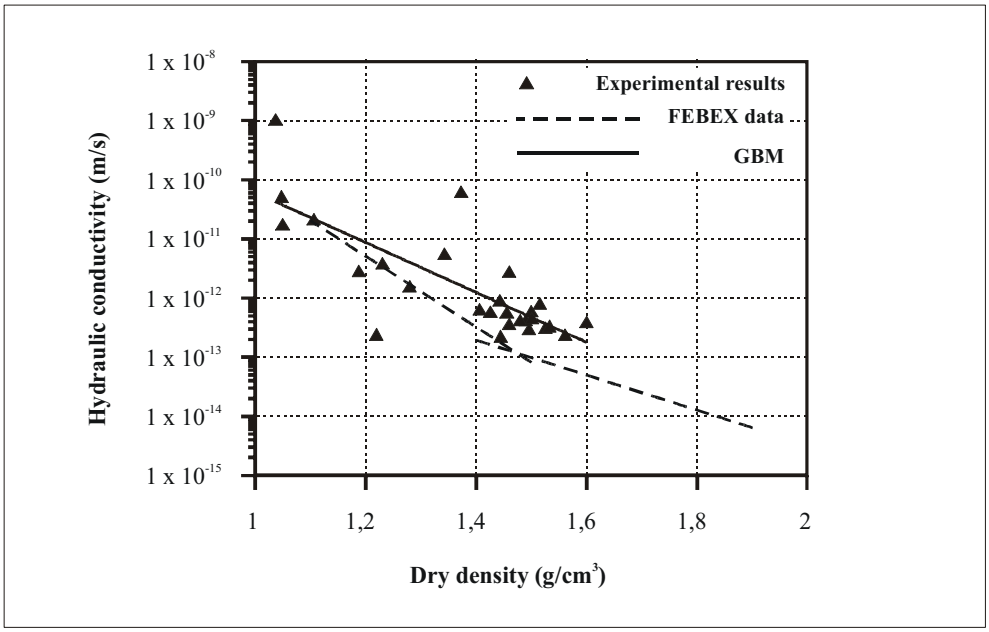

Figure 17: Hydraulic conductivity values of pellet samples at different dry density values. Saturated conditions

Infiltration tests were also performed to study the relationship between hydraulic conductivity and degree of saturation. Water was injected into the samples while the volume was kept constant. Tests were grouped considering sample characteristics, dry density, grain size distribution, initial water content and the water injection history. Within each group tests with different infiltration times were performed, which could be considered as a unique test. The water content distribution along the sample, at different times, could then be established and interpreted using "back analysis" techniques. Parameters obtained for the infiltration tests performed on samples with dry density values of 1,5 g/cm^3 are presented in Table 3.

Table 3: Parameters obtained for the relative permeability law. ρd =1,5 g/cm^3

Relative permeability law	Parameter values
$k_r = A \times S_r^{\lambda}$	A=1, λ=1,8

3.3.2 Mechanical properties

Oedometer tests under saturated conditions; oedometer tests under constant suction; wetting under constant load tests (liquid water was used); swelling pressure tests; suction controlled wetting under constant load tests and suction controlled wetting at constant volume tests were performed on samples with dry density values varying between 1,3 to 1,9 g/cm^3.

Compressibility

Loading-unloading paths at constant suction were performed. First, the saturated condition was investigated and then additional tests were performed under suction control. Stress paths followed during these series of tests are shown in Figure 18. Based on these tests, the elastic and plastic compressibility moduli ($\kappa(s)$ and $\lambda(s)$ and the elastic load limit ($\sigma_v(s)$), which defines the LC yield surface, were obtained. Derived parameters are presented in Table 4.

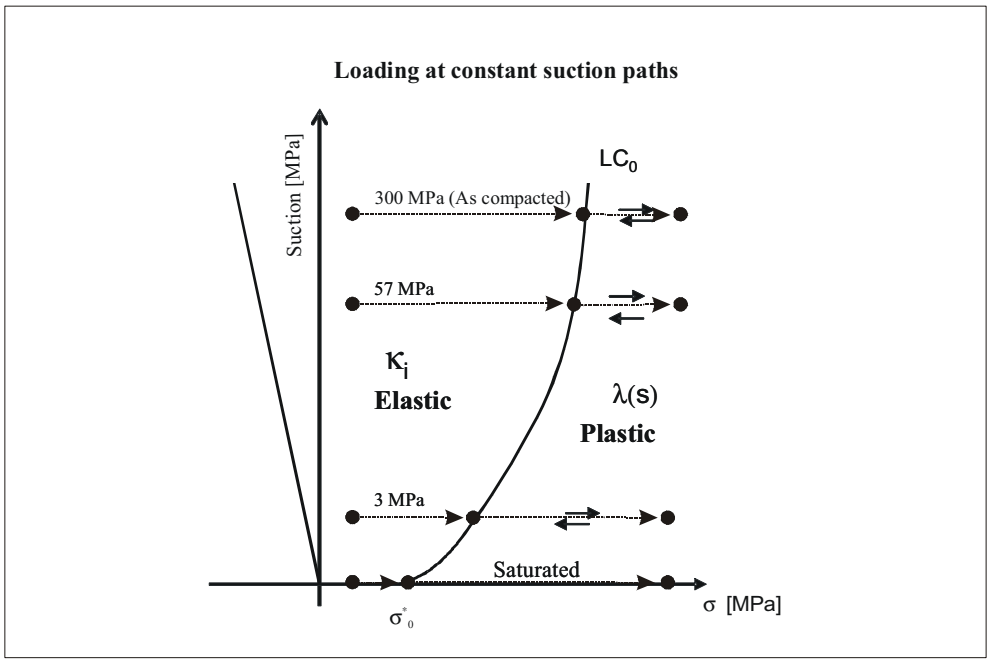

Figure 18: Stress paths applied in compressibility tests

Table 4: Compressibility parameters for two dry densities: 1,3 and 1,5 g/cm^3

Elastic Parameters - $\kappa_i(s) = \kappa_{io} * (1 + \alpha_i * s)$				
Parameter **Dry density**	$\kappa(300)$	$\kappa(57)$	$\kappa(3)$	κ_0
1,3 g/cm^3	0,01	0,045-0,07	0,055	0,08-0,11
1,5 g/cm^3	0,0045	0,025	0,035	0,060-0,070
Elastic limit [MPa]. (Yield surface- σVx(s))				
(*) 1,3 g/cm^3	2,0	0,80	0,75	0,65-0,70
(*) 1,5 g/cm^3	5,0-6,0	2,8-3,0	2,8-3,0	1,35
Plastic parameters - $\lambda(s) = \lambda(0)[(1-r)\exp(-\beta s) + r]$				
Parameter	$\lambda(300)$	$\lambda(57)$	$\lambda(3)$	λ_0
1,3 g/cm^3	0,022-0,027	0,155	0,163	0,175-0,188
1,5 g/cm^3	0,018-0,022	0,133	0,140	0,160-0,173

Wetting under constant load

Samples were statically compacted and then installed in an oedometer cell. Samples were first loaded and then soaked with synthetic formation water. Measured swelling deformations as a function of vertical load and initial dry density are given in Figure 19. Integrating all test results, an empirical relation between volumetric swelling, vertical load and dry density could be derived:

$$\frac{\Delta H}{H_0} = -0{,}0939 \times \ln(\sigma) + 0{,}732 \times \rho_d - 0{,}4161$$

where [σ]= kPa and [ρd]=Mg/m3. Setting $\Delta H / H_O = 0$ in the previous expression yields:

$$\sigma(\rho_d) = 0{,}0611 \times e^{6{,}744\rho_d}$$

This equation provides a lower limit for the swelling pressure of the material. Stress paths which not activate the Load Collapse yield surface, were used to obtain information on the elastic domain. Parameters obtained are shown in Table 5.

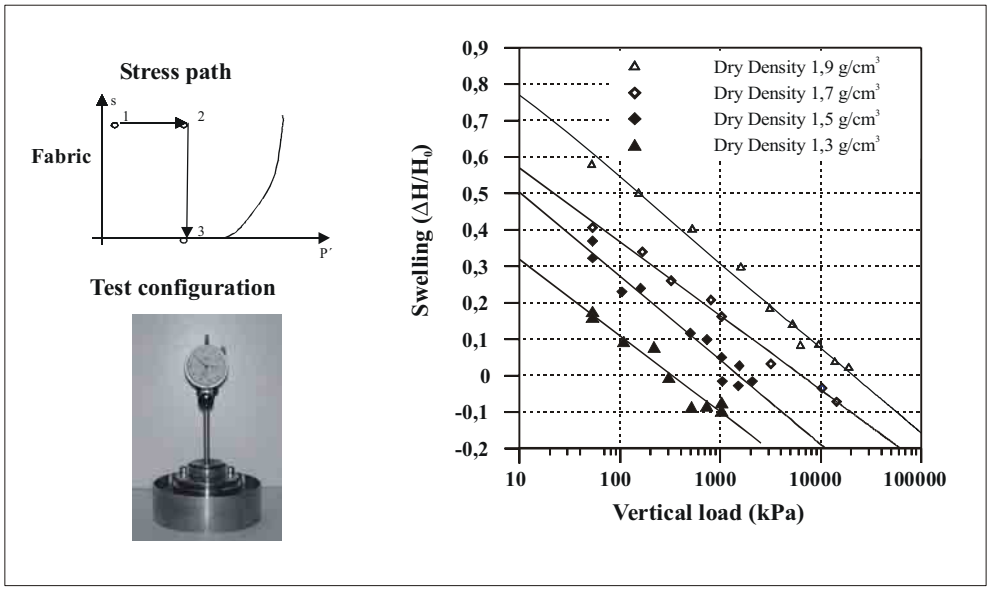

Figure 19: Wetting under load tests. Stress path, test configuration and results obtained

Table 5: Parameters obtained from wetting under constant load tests

1,3 g/cm^3		**1,5 g/cm^3**	
Load at fabric conditions $\kappa_i(s) = \kappa_{io} * (1 + \alpha_i * s)$			
ki(s)	kio(1+αi*S)	ki(s)	kio(1+αi*S)
kio	0,08	kio	0,065
α_i	-0,00274	α_i	-0,0031
Load at fabric conditions $\kappa_s(p', s) = \kappa_{so} * \left[1 + \alpha_{sp} * Ln\left(\frac{p'}{\mathrm{Pr}}\right)\right] * e^{\alpha ss * s}$			
kio	-0,063	kio	-0,11
□sp	-0,181	□sp	-0,183
□ss	0,003	□ss	0,001

Wetting at constant volume (swelling pressure tests)

Samples were saturated at constant volume (synthetic formation water was used) and the swelling pressure monitored. First an elastic swelling is recorded but, when the stress path reaches the yield surface LC, some collapse is observed. Final swelling pressure values are shown in Figure 20. The empirical relation obtained for compacted natural Febex bentonite is also plotted. A good agreement is observed. The relationship between swelling pressure and dry density can be written as:

$$\sigma_V(\rho_d) = 0.00037 * e^{5.9\,\rho_d}$$

where $[\sigma_V]$=MPa, $[\rho_d]$=g/cm^3

Some difference between swelling pressure values obtained in the wetting under load tests and the swelling pressure tests was observed. Lower swelling pressure values were recorded in the wetting under load tests, a result which can theoretically be explained.

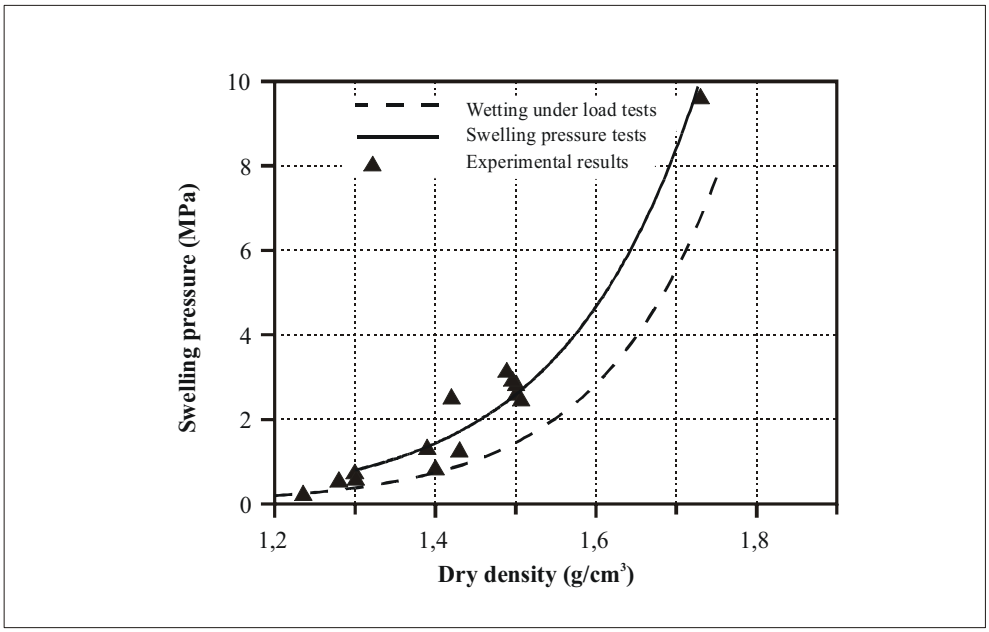

Figure 20: Swelling pressure results obtained in wetting at constant volume tests

Vapour and liquid transfer tests. Wetting under constant load.

Two different wetting techniques were used to perform swelling under load tests following the same suction-stress path in a suction controlled oedometer. The first technique involves saturation with liquid water. In the second case, a vapour equilibrium technique was used. In both tests, the applied vertical confining stress was kept equal to 300 kPa. Stress paths are shown in Figure 21.

In the test involving wetting with liquid water, the stored water volume was controlled and suction values were derived from the water retention curve. In the second test performed, the wetting path was followed in a step-by-step process by varying the chemical potential of different types of aqueous solutions used to control the relative humidity of the air circulated through the specimen. Each suction step was maintained until no volume change was registered in the sample. Once a minimum suction value of 3 MPa was reached, liquid water was finally injected to achieve the saturated condition.

A different behaviour was observed in both tests during the saturation process (Figure 21). When liquid water was injected an initial collapse was observed immediately after inundation. Then, the expanding granules started to swell and a net swelling deformation was measured. At a final stage, however, when the specimen was close to saturation, additional collapse deformations were registered. In the vapour transport case a net swelling deformation (volumetric expansion) was measured from the very beginning of the test and for all the subsequent vapour equilibrium stages until a suction value of 3 MPa was reached. Then, at the final stage, when liquid water was injected to bring the suction to zero, a sudden collapse was initially observed followed by some final swelling deformations. These results show that during the wetting process different constitutive behaviours are susceptible to occur depending on the water transfer mechanism.

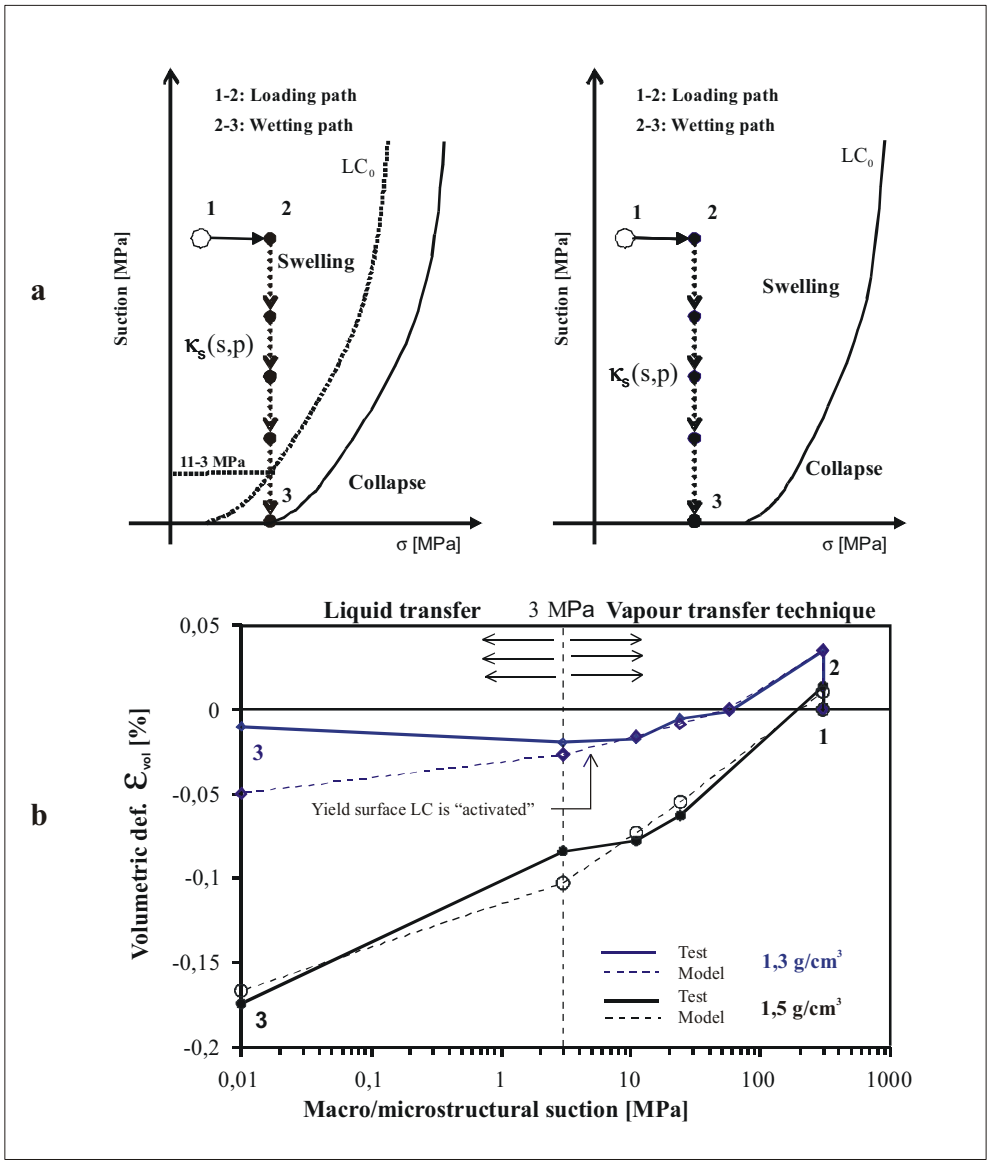

Figure 21: (a)- Stress paths for wetting under constant load tests performed over samples of 1,3 and 1,5 g/cm^3. (b)- Test results and model predictions obtained for these tests

Model predictions were obtained considering the GBM as an ideal elastic material. Volumetric deformations were calculated based on parameters previously determined. Good agreement was observed between experimental results and model predictions in test corresponding to a dry density of 1,5 g/cm^3. The initial position of the yield surface LC and its subsequent hardening could be determined in these tests.

Vapour and liquid transfer tests. Wetting under constant volume.

In tests involving liquid wetting, samples were soaked with synthetic formation water and the incoming water volumes and the vertical swelling pressure were monitored. In these tests suction was derived from the water retention curve of the material. In the case of wetting with the vapour equilibrium technique, the relative humidity of the air circulated through the sample was controlled by means of different aqueous solutions until a relative humidity corresponding to a suction value of 3 MPa was reached. At this time and in order to achieve full saturation of the sample, liquid water was injected. Special oedometer cells were designed and built in order to perform the vapour controlled tests (Figure 22). In these cells a constant volume condition was maintained and swelling pressure was measured by means of a load cell

which blocks the upward movement of the sample load cap. Water content was controlled by weighing the testing cell in an electronic balance. Each suction step was maintained until neither water content nor vertical swelling pressure changes were registered in the sample.

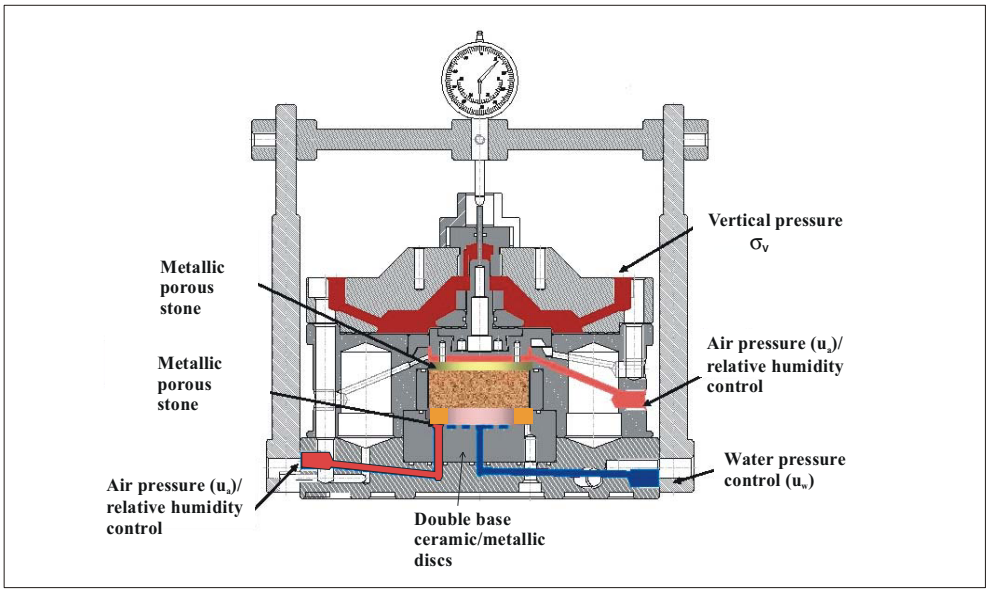

Figure 22: Oedometer cell specially designed to perform suction controlled swelling pressure tests. Suction can be controlled in the range: 300 MPa to saturation

The wetting technique affects the recorded swelling pressure development (Figure 23). This can be explained because of the double structure nature of the material. Both structural levels have very different water permeability so when liquid transfer is used, the water goes into the sample through the macropores making the suction to decrease at this structural level while the suction at microstructural level remains almost constant. On the other hand, if vapour transfer is used, slower wetting rates are applied and the suction at both structural levels evolves in equilibrium during wetting. Water absorbed by the large pores will not produce major swelling but swelling is observed as the microstructural level becomes saturated. If vapour is used the microstructure incorporates water at early times of the test and a swelling pressure develops steadily as the suction decreases.

Effect of imposed gradient on swelling pressure tests.

Two tests were performed to study the effect of the imposed gradient on the swelling pressure. Liquid transfer was used and a single wetting step to saturation was applied. Two boundary pressures were applied: 20 kPa and 200 kPa. In both specimens the dry density was kept constant (1,3 g/cm^3) and the swelling pressure was monitored. The water content was measured and suction was derived from the water retention curves.

Widely different results were obtained. The observed behaviour can be interpreted with the help of a double structure model: When water is stored in the macropores, very little or almost null swelling is likely to occur. On the contrary, a strong swelling will probably occur as the microstructural level becomes hydrated. The different evolution of degree of saturation explains the different reactions of the mixture in both tests (Figure 24).

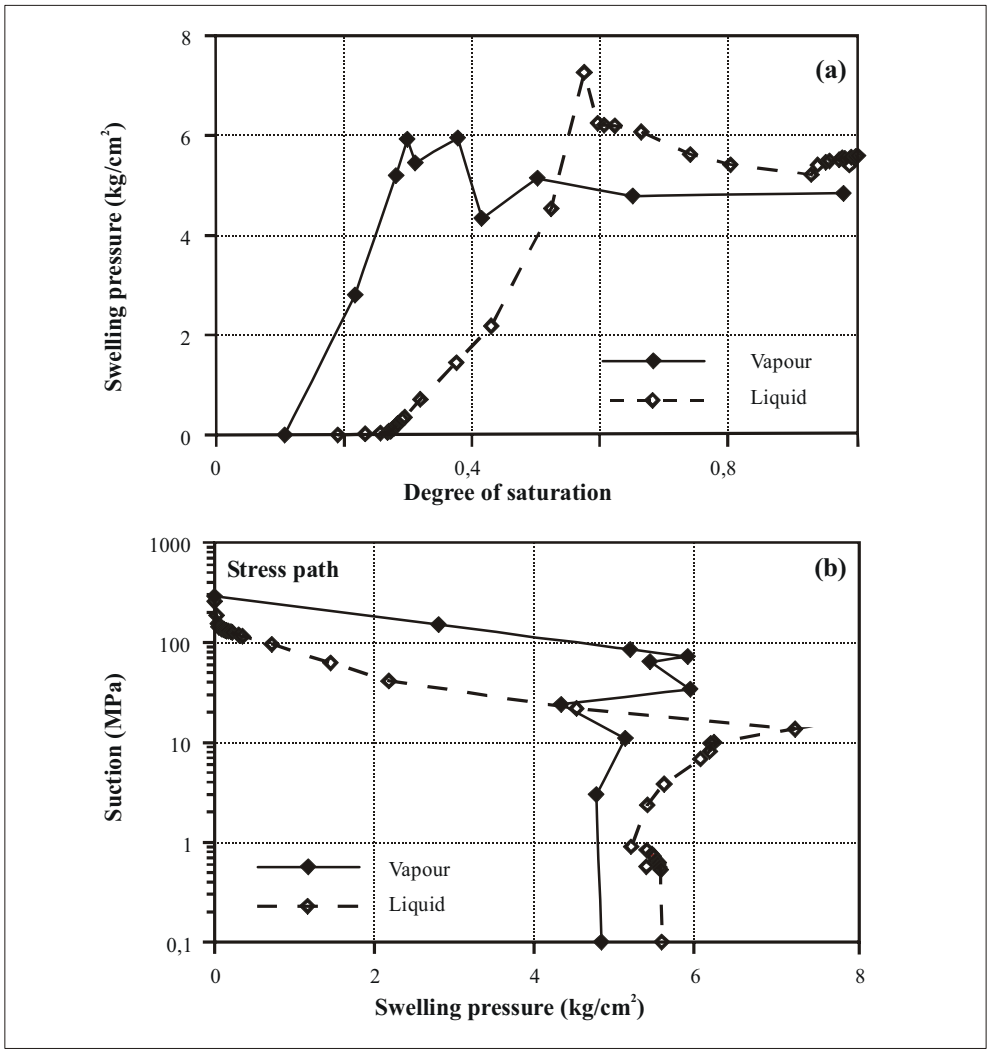

Figure 23: Constitutive response of the pellet mixtures during wetting at constant volume. Tests performed with vapour and liquid transfer. (a)- Evolution of the swelling pressure with the degree of saturation. (b)- Stress path described in terms of vertical swelling pressure and suction

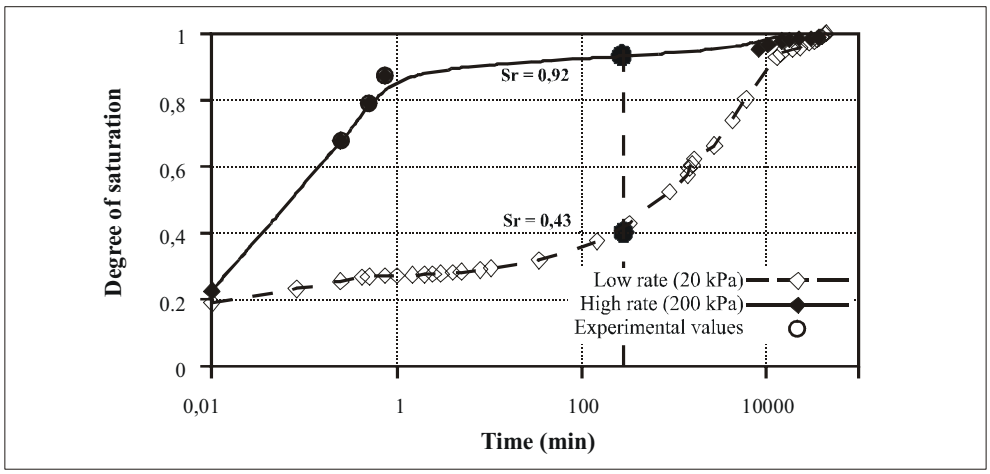

Figure 24: Time evolution of the degree of saturation during swelling pressure tests with different water injection gradients

3.4 GBM laboratory seismic characterization

The development of seismic velocities and amplitudes of seismic waves was determined as functions of hydration of the backfill. Tests were performed on cylindrical samples of bentonite pellets as used for backfilling. The bentonite pellets were poured in Plexiglas cylinders with an inner diameter of 50 mm to a height of 100 mm. The obtained dry density was 1,45 g/cm^3. Piezo-transducers were attached to the Plexiglas cylinders to measure the seismic velocities across the samples. This assembly was mounted into a triaxial pressure vessel. Axial length of the specimen was kept close to constant. Radial deformation was inhibited by the Plexiglas tubing and by adjusting the confining pressure to the axial pressure. Distilled water was injected from the bottom of the sample with a back pressure of 6 bar (Except sample 5 with only 2 bar backpressure). Initial fast flushing of the pellets was obtained by evacuating the samples prior to first water injection.

Figure 25 shows the general testing procedure: Previous to flushing the confining pressure was adjusted to about 5 bar. With first flushing about 60 to 75 ml water flew into the sample (blue line). Then the axial pressure increased due to swelling (red line) and the confining pressure (green line) was adjusted in such a way that it always stayed well above the axial pressure. Lower confining pressures caused dilation of the sample and finally rupture of the Plexiglas tubing. Maximum axial pressures achieved after 80 days ranged between 20 and 30 bar. (Except for sample 5 where only 14 bar were reached with 2 bar backpressure).

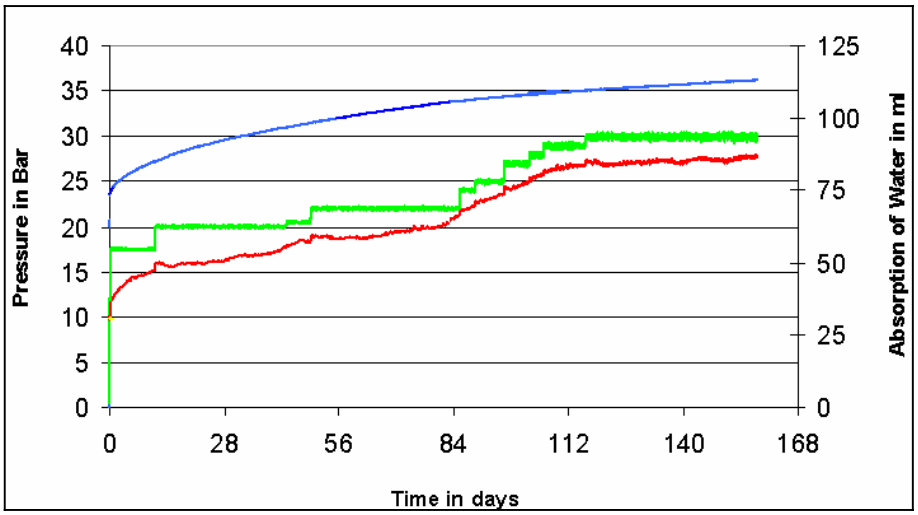

Figure 25: Figure BGR1: Water inflow (blue; right scale), axial pressure (red; left scale) and confining pressure (green; left scale). Data are given for Test No. 10

Seismic velocities were measured during hydration across the sample. Figure 26 shows the first 120 µs of the transmitted seismograms. The amplitudes are colour coded. Seismograms are given for the first 70 days of test No. 10. It is obvious that the amplitudes increased tremendously during the first 40 days of hydration and then reached an almost constant level. The travel times decreased during the same time interval. The evolution of the signals indicates an increasing homogenisation of the backfill material.

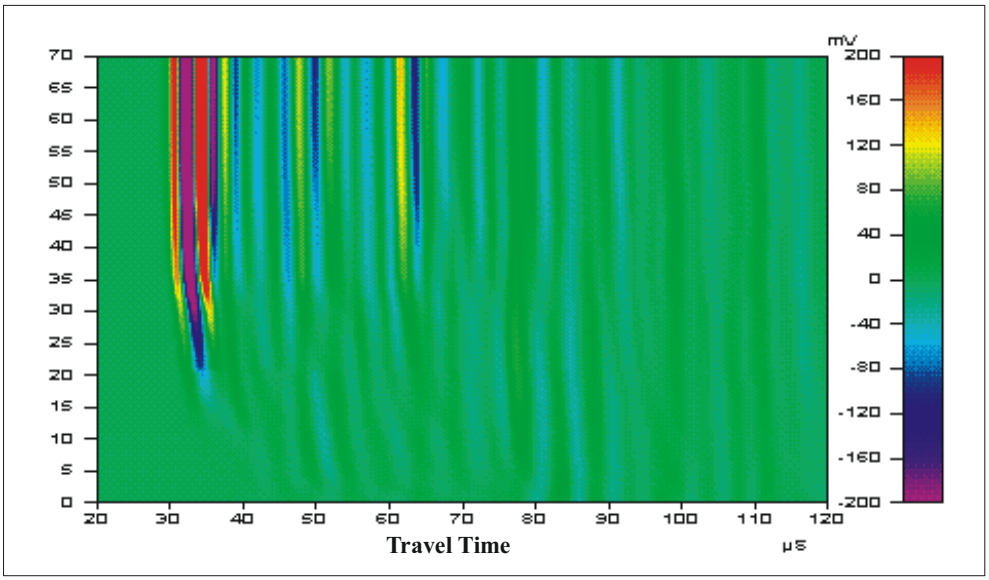

Figure 26: The first 120 µs of the received seismograms. The amplitudes are colour coded. Seismograms are given for the first 70 days (vertical axis) of test No. 10

All in all 6 samples were tested. Test durations ranged between 40 (failure of Plexiglas tube) and 160 days. With the first two samples the seismic transducers were installed 5 cm above the bottom of the sample. This means the velocities and amplitudes were measured 5 cm in front of the water injection area. The results from these samples are given in black and grey in Figure 27 and Figure 28. In later tests the transducers were mounted only 2,5 cm from the bottom of the samples. These results are given with coloured symbols in Figure 27 to Figure 29.

Figure 27 shows the changes in p-wave velocity with increasing absorption of water. It is obvious that at a distance of 5 cm the initial velocities right after flushing and the velocity changes are much lower than at a distance of 2,5 cm. In addition the results at 2,5 cm indicate a maximum velocity of about 2000 m/s. The differences in seismic wave transmission at different distances to the water injection area are even more pronounced in the amplitudes (Figure 28). At a distance of 5 cm almost no amplitude increase was observed. Only after injection of 120 ml of water the amplitudes started to increase slowly. At 2,5 cm the amplitudes showed a significant increase already after injection of 80 to 90 ml of water.

Figure 29 summarises the results for a distance of 2,5 cm. Initially the velocities increased without significant increase of amplitudes. Then amplitude increase starts and continues even after the maximum velocity of 2000 m/s has been reached.

The results show, that the saturation front moves rather slowly. Even with a back pressure of 6 bar and an injection across the total base of the specimen (not a line source as in the EB-tunnel) maximum velocities were only reached after 40 to 60 days at a distance of 2.5 cm. At a distance of 5 cm these velocities were not reached even after 90 days.

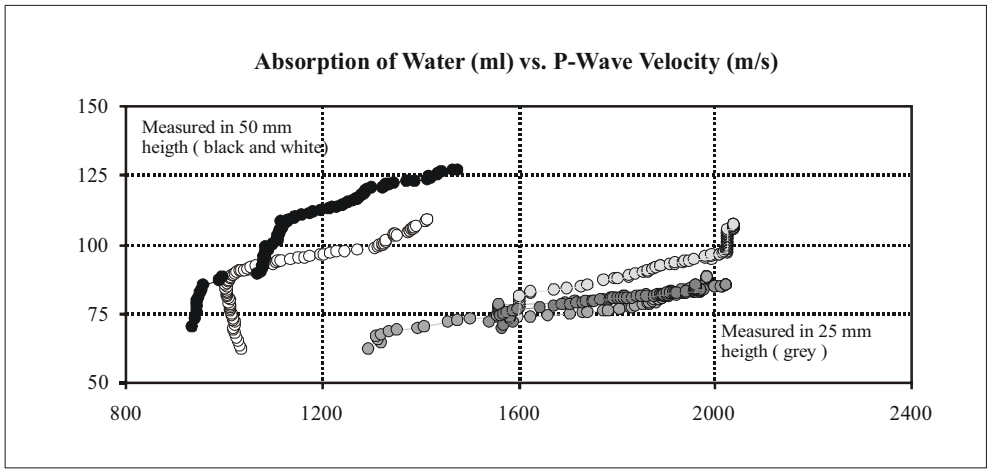

Figure 27: Water inflow vs. p-wave velocity. (White: sample 5 with only 2 bar back pressure)

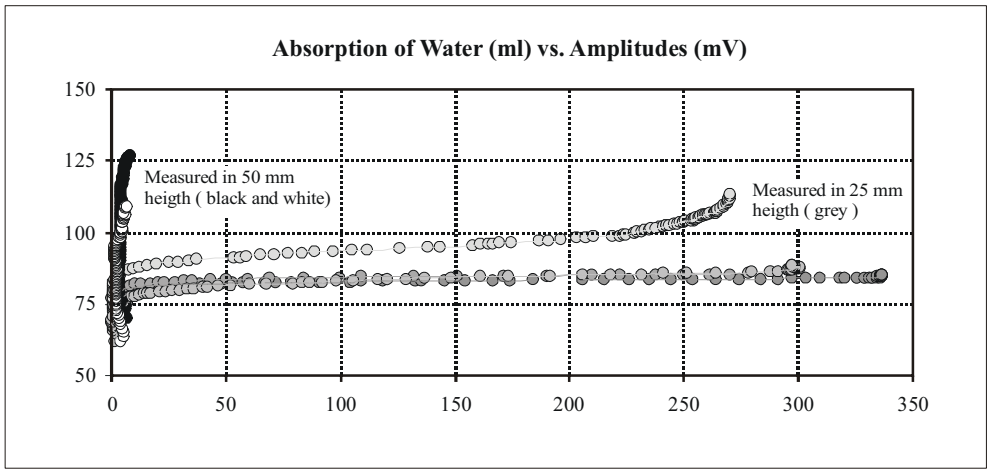

Figure 28: Water inflow vs. amplitudes of seismic waves. (Grey: sample 5 with only 2 bar back pressure)

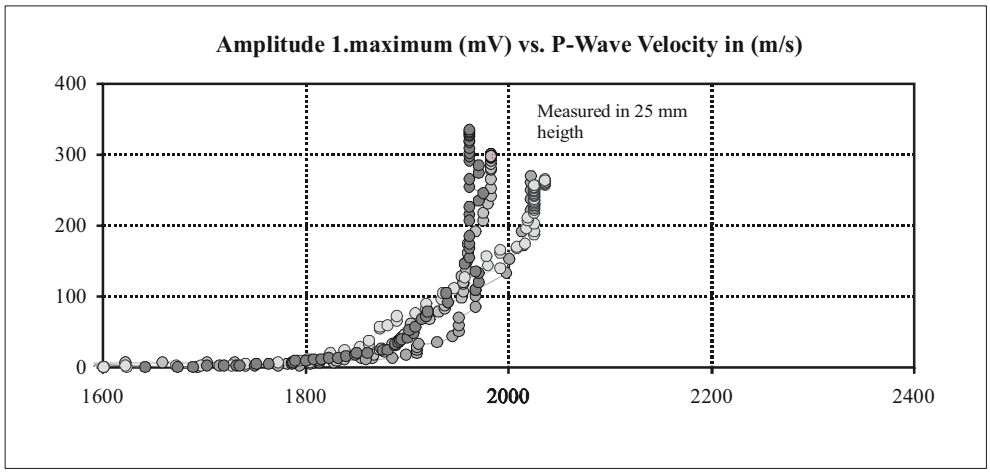

Figure 29: Amplitudes of seismic waves as functions of p-wave velocities

4 DRIFT EXCAVATION AND CHARACTERIZATION

4.1 Drift excavation

Excavation of the EB niche started on 2nd of April 2001. Initially 9m had been excavated with a pneumatic hammer till 27th of April 2001. This first 9 m of the tunnel were shotcreted. Excavation of the last 6 m (the planned experimental area of the EB-experiment) started on 15th of May 2001. This part was excavated by a modified road header to guarantee a profile with a tolerance of ± 5 cm. During a first step, a smaller profile was excavated from 9 to 15 m. The final profile was obtained in a second step, where special emphasis was taken for keeping the prescribed tolerance of plus/minus 5 cm (deviation from ideal profile). The small-profile excavation from 9 - 15 m with the road header has been completed on 23rd of May. To guarantee the tolerance of ± 5 cm the two frontal head-cutters of the road header were replaced by a smaller single head. Excavation was successfully finished by 8 June 2001. Geological documentation has been carried out in the whole tunnel. Finally the tolerance was controlled by a 3D laser scanning (Figure 30). Note the differences in surface roughness between the first part excavated by pneumatic hammer and the deeper part excavated in two steps by road header.

Figure 30: 3D Laser Scan Cyrax® 2500. Overview of whole EB niche, frontal and rear part

4.2 Geophysical characterization of EDZ

High frequency seismic and geoelectric in situ measurements were performed in summer and autumn 2001 respectively. The results from these geophysical and additional hydrogeological testing define the initial conditions for the long-term monitoring during the hydration of the rock and the backfill materials. The measuring points of the different methods are placed very near to each other but at a distance where no interaction is assumed (Figure 31).

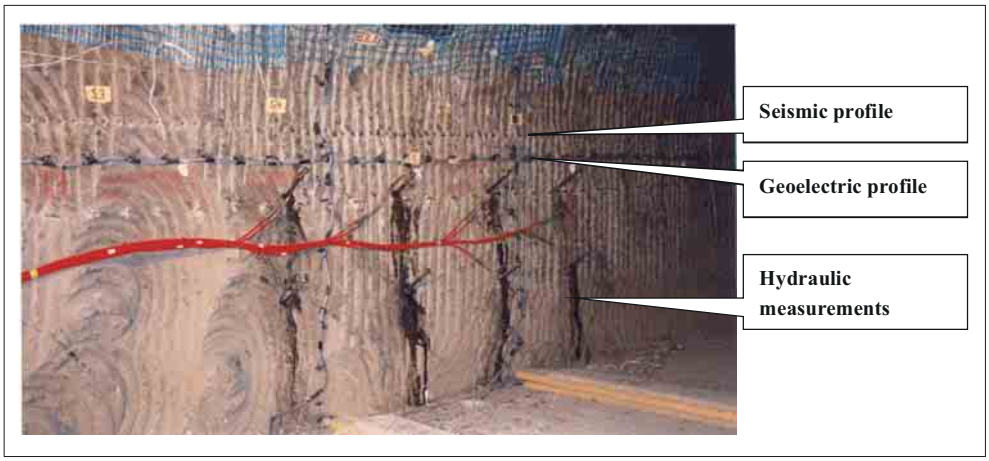

Figure 31: Locations of horizontal seismic and geoelectrical profiles and positions of the hydrogeologic measurements

4.2.1 Seismic measurements

Aim of the investigation was the determination of the extent of the EDZ. Different seismic techniques were applied during two measurement campaigns in June and October 2001. A mini-sonic borehole probe was used for the interval velocity measurements along six radial 3 m long boreholes in two planes. Both planes are 1 m apart. Furthermore cross hole and seismic tomography measurements between two boreholes were carried out. Along the walls of the EB niche three seismic refraction profiles with lengths of 1,9 m, 2,5 m and 5,6 m were measured. Repetition of measurements after four months offered the opportunity for an assessment of the change of seismic parameters.

The EDZ was characterised with the help of seismic parameters like P- and S-wave velocities as well as their amplitudes derived from interval velocity measurements. According to these results the extent of the EDZ varies between 0,10 m (sidewall), 0,5 m (roof) and 0,65 m in-between (45° inclined boreholes). A compilation of the results is given in Figure 32. The differences of the extents of the EDZ between June and October 2001 are too small to be significant.

Nevertheless, changes in the derived P-wave velocities after four months indicate local stress redistributions. According to increased and decreased P-wave velocities a gentle loosening of the rock was observed in the roof and a consolidation in the 45° inclined boreholes. In the subhorizontal direction up to 0,6 m the rock seems to be loosened and for greater depth more consolidated.

Increased P-wave velocities in the sidewalls at a depth between 0,3 and 1,0 m correlate with sandy layers identified in the core samples. Dynamic elastic parameters were calculated from the data.

A distinct anisotropy of seismic velocities, which can not be exclusively explained by the bedding of the Opalinus Clay, was revealed with the help of cross hole measurements. Dependent on the travel paths of seismic waves the derived P-wave velocities vary between 2200 m/s and 3100 m/s.

Results from seismic refraction measurements along a 5,6 m long horizontal profile at the NE sidewall show the EDZ as a thin layer (0,05 – 0,15m) with varying velocities between 900 m/s and 1400 m/s. The velocities of the undamaged rock vary between 2300 m/s and 3000 m/s. Discontinuities in the related travel time curves correlate with mapped structural elements. Results from all three seismic methods are in good agreement.

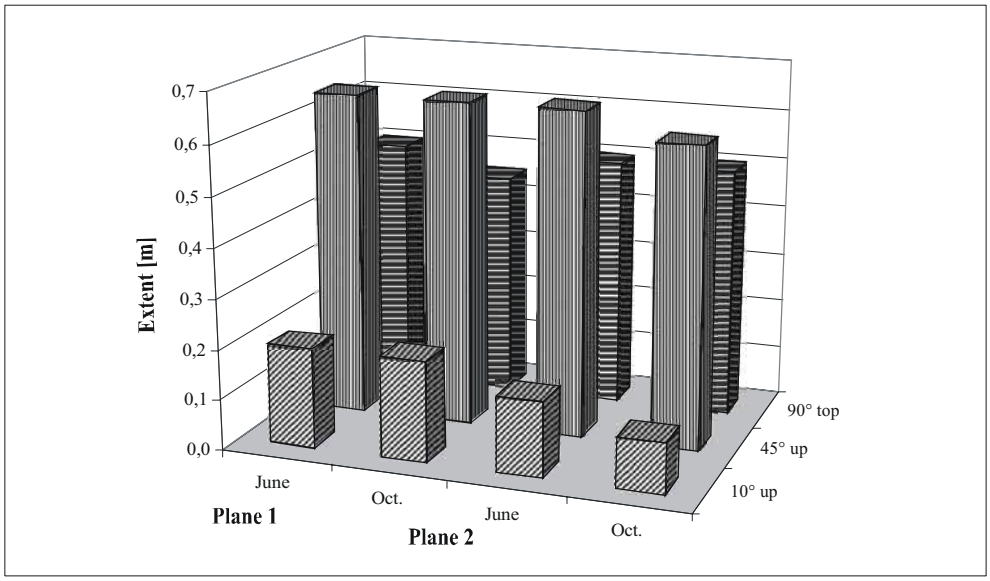

Figure 32: Extent of the EDZ for boreholes in plane 1 (BEB-B09 – BEB-B11, left side) and plane 2 (BEB-B19 – BEB-B21, right side)

4.2.2 Geoelectric measurements

Three field surveys provided the data basis for the geoelectrical assessment of the EDZ. The first campaign took place in July, the second in September and the third in October 2001. Thus, a rather detailed monitoring of extent and temporal behaviour of the electric rock properties was possible.

In repeated measurements it proved that undamaged Opalinus Clay in the EB-Niche has a resistivity of around 8 Ωm and a phase around –0,4. In July the EDZ emerged as an 0,75 meter thick rock region in the tunnel roof, where resistivities up to 64 Ωm and only phases around –0,2 were measured. The later measurements showed an enlargement of the EDZ mainly in the roof. In September and October its thickness reached nearly 1 m. At the sidewalls a zone of increased resistivities was found up to a depth of 0,10 to 0,15 m. A second zone of high resistivities in combination with high phase values, was found in the tunnel wall at a depth of about 0,4 to 0,5 m. In the July measurement this phenomenon was most ostentatious, whereas it decreased somewhat in the later measurements.

As an example results of the resistivity distribution along the annular profile 1 is shown in Figure 33.

Laboratory geoelectric measurements permitted the correlation of different resistivities to particular water contents (saturations). The unaffected Opalinus Clay, which is typically 8 Ωm, is fully saturated, whereas the EDZ featured resistivities between 16 and 60 Ωm.

4.2.3 Conclusions

The geophysical characterisation shows a clear identified EDZ in the roof up to a depth of about 0,7 m. At the sidewalls the EDZ reaches a depth of about 0,1 m. Indicators for the EDZ are low velocities, low amplitudes, high resistivities and small phases. In the roof a slight increase in the extent of the EDZ with time was observed by geoelectric measurements, the seismic measurements, however, showed no geometrical increase of the EDZ but an increased damage with time.

At the sidewalls a combination of high velocities, high amplitudes, high resistivities and small phases characterises a zone at depths between 0,3 and about 1,0 m. The results of the measurements are in this case not typical for the EDZ neither for the intact rock. The anomaly may be due to sandy layers observed

at that specific depth and/or to stress concentrations induced by the drift itself which results in a slightly squeezed material.

Seismic and geoelectric measurements resulted in qualitatively similar and mutually complementing characterisations of the EDZ.

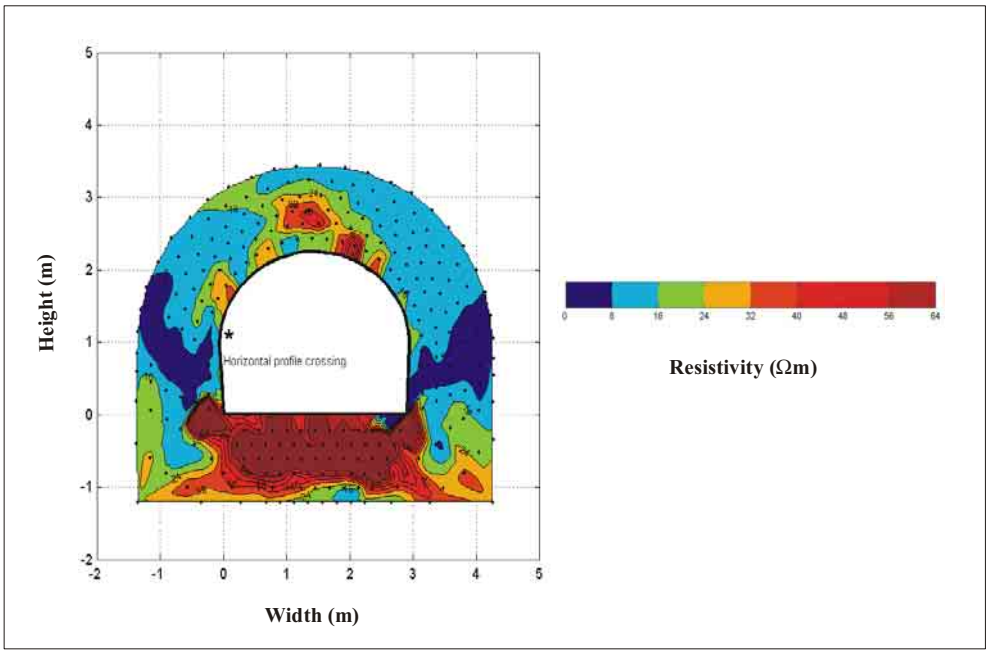

Figure 33: Inversion results of geoelectrical annular profile 1. Distribution of specific electrical resistivity (undisturbed or only slightly disturbed Opalinus Clay: < 16 Ωm, concrete: > 200 Ωm, EDZ: 16 - 60 Ωm)

4.3 Hydrogeological characterization of EDZ

The initial hydrogeological characterization has been performed in two campaigns in October 2001 (Phase 1) and April 2002 (Phase 2). The boreholes were drilled to depths of approximately 0,3 to 0,9 m at an angle of 30° from the horizontal. The boreholes have a diameter of 30 mm and were drilled using an air-rotary drill. The schematic borehole configuration is shown in Figure 34. The borehole identifications were modified after the first hydraulic test series the figure shows the new as well as the initial numbering. Pneumatic extraction tests were performed initially during Phase 1 to obtain a rough permeability estimation, that was used as criteria for the hydraulic test design and to detect possible cross hole responses. Then a first saturation of all boreholes was performed. About a week later hydraulic constant head/rate injection testing and hydraulic pulse testing were conducted. The second hydraulic test series (Phase 2) was performed immediately after completion of the sealing plug.

Both campaigns showed the highest permeability at a distance of about 50 cm from the tunnel wall. The hydraulic conductivity obtained in the boreholes BEB-6 and BEB-17 using the pulse test data in April 2002 ranges between about 5 x 10^{-12} and 1 x 10^{-11} m/s. The results are significantly smaller than the estimates obtained from first hydraulic test series in October, 2001 (5 x 10^{-11} and 6 x 10^{-11} m/s). The estimates from the constant head tests in boreholes BEB-4, BEB-5, BEB-14 and BEB-15 (except borehole BEB-16) were approximately one order of magnitude smaller than the results from first hydraulic test series (4 x 10^{-10} and 9 x 10^{-9} m/s compared to 1 x 10^{-10} and 8 x 10^{-10} m/s).

The observed decrease of permeability in the EDZ after resaturation in the vicinity of the test holes agrees well with earlier test results from the EH-experiment at Mont Terri. The decrease may have resulted in

the absence of observed crosshole responses in most of the boreholes where, during the first hydraulic test series with similar testing times, slight pressure responses had been observed.

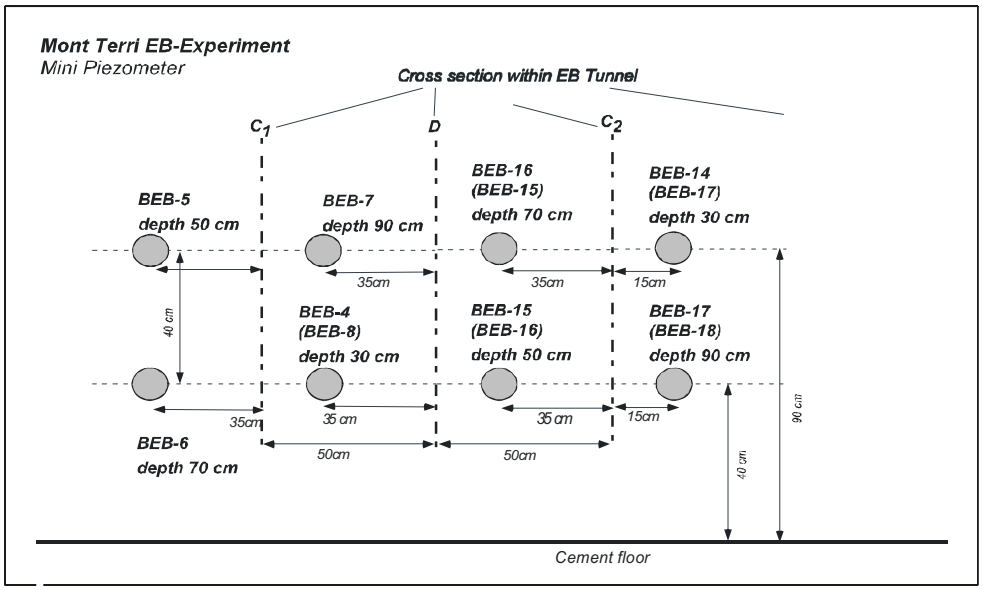

Figure 34: Schematic borehole configuration (old identifications indicated in brackets)

Hydraulic conductivity (K) estimated from the tests performed in borehole BEB-7 indicate a difference of about 1,5 orders of magnitude in Phase 2. The pulse test data yielded a hydraulic permeability of about 3 x 10^{-9} m/s compared to about 7 x 10^{-11} m/s with the constant head test data. The characteristics of the hydraulic pulse test response and the fact that the transmissivity obtained with the pulse test data is higher than the transmissivity obtained with the constant head data indicate the possibility of a negative skin effect around the borehole.

The results of these test series indicate that constant head injection tests should be the preferred hydraulic test type in the EDZ. Additionally, the acquisition of new test equipment by Solexperts (new flow meter/controller with a low measurement limit of 5 µl/min) had improved the performance of constant head injections tests in the BEB boreholes. Figure 35 shows the permeabilities measured during the two campaigns as a function of depth from the tunnel wall. Results are only shown for constant head tests.

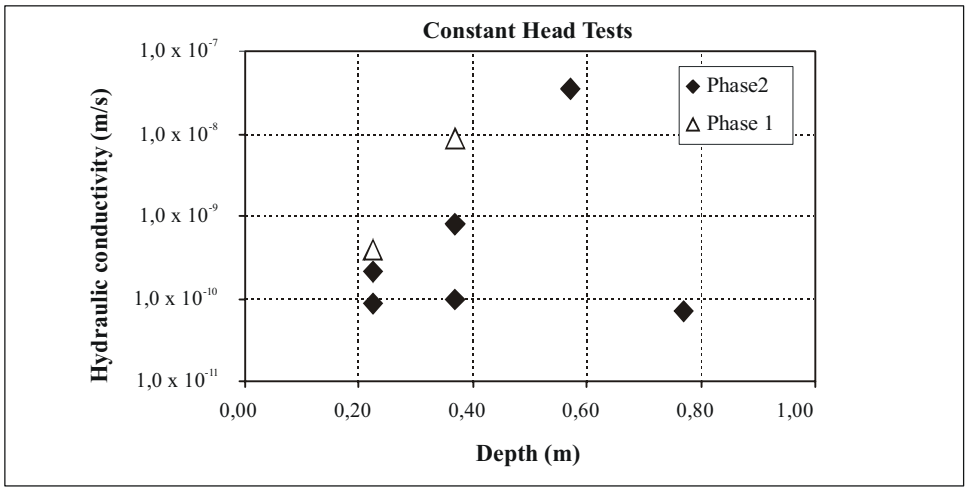

Figure 35: Hydraulic conductivity measured during the two campaigns as a function of depth from the tunnel wall. Results are only shown for constant head tests

5 TEST CONSTRUCTION

5.1 Canister and bentonite blocks bed

Bentonite blocks were delivered to the site to construct the base of the bentonite buffer. They were supported by the concrete bed (Figure 36 and Figure 37). The canister fits exactly into the radial section of these blocks.

The bentonite bed (three layers of blocks) has a nominal thickness of 66 cm. A total number of 36 bentonite blocks were required.

A specially designed high-capacity, low-height equipment transporting trolley positioned the canister in the exact position over the bentonite blocks (Figure 36). The canister was temporarily secured with a support system and filled with a high density fluid to its target weight.

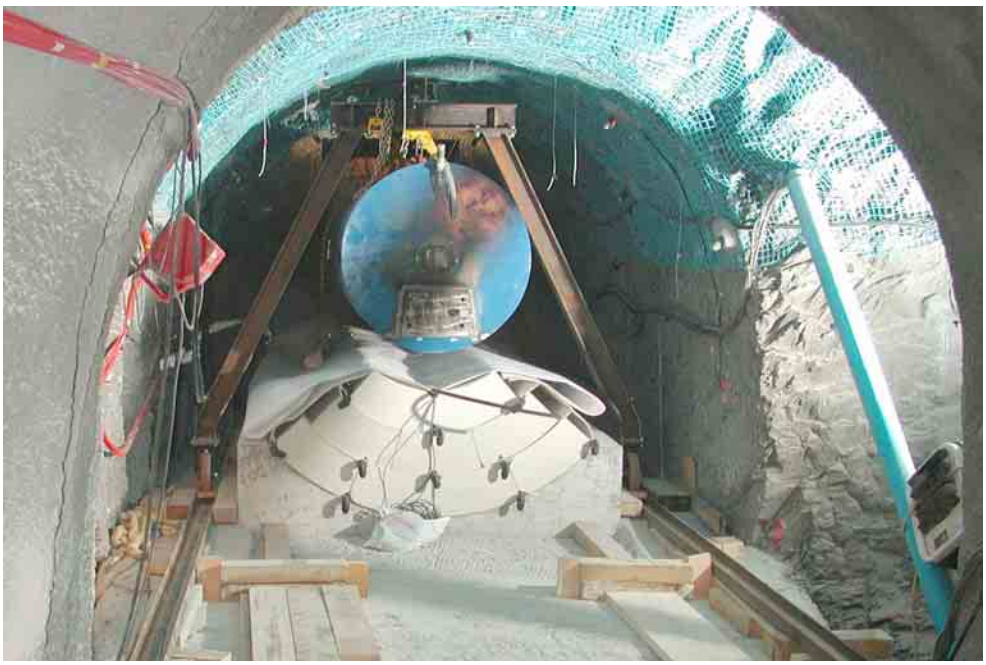

Figure 36: Placement of the dummy canister on the betonite blocks which are supported by a concrete bed

5.2 Installation of hydration system and instruments

After the excavation of the niche, the rock instrumentation was installed: seismic instrumentation first, then the hydrogeological one and finally the hydromechanical ones (piezometers, relative humidity sensors and rock extensometers).

A total of twenty three boreholes were drilled in the rock around the test section for rock instrumentation purposes. According to their type, sensors are grouped as follows:

- Relative humidity and temperature: four boreholes
- Pore pressure: fourteen boreholes
- Rock displacement: three boreholes
- Seismic characterization: two boreholes

Boreholes for instrumentation have different diameters depending on the type of sensor installed. The installation of these sensors took place in November 2001.

On the other hand, in the buffer (blocks and GBM), eight total pressure cells, four extensometers and eight relative humidity sensors were installed.

As the idea was to hydrate the buffer artificially, some distribution pipes and hydration mats had to be installed into the bentonite blocks. Therefore, some of the bentonite blocks were cut to allocate these tubes. Five double hydration mats, made of a special geotextile fibre, were also installed. The two first mats were placed under layer #1 of bentonite blocks, directly over the concrete bed. The third mat was installed between layers #1 and #2 and another one was placed on top of bentonite blocks. The last mat was sewed around the canister (Figure 37).

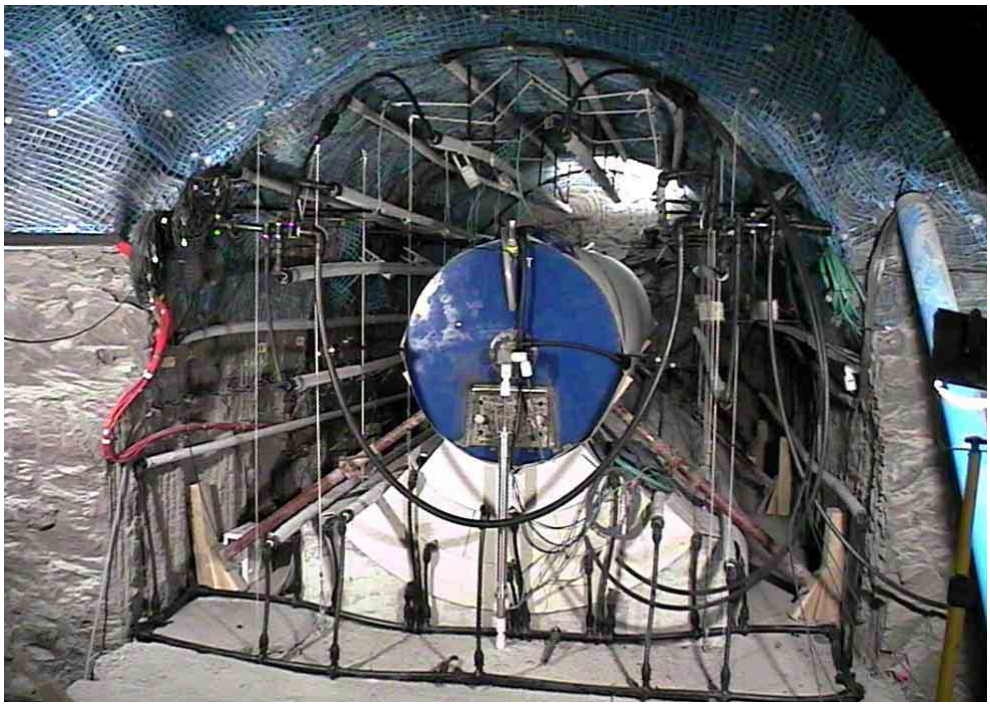

Figure 37: Pre-conditions of the GBM emplacement

5.3 GBM emplacement

Seven activities took place for the emplacement of the GBM.

1. Equipment and bentonite delivery
2. Equipment and infrastructure installations and modifications
3. Bentonite weighing and sampling for quality assurance
4. Bentonite sample analyses
5. Bentonite emplacement
6. Retaining wall sealing
7. Equipment removal and site cleanup

The equipment was delivered by Gasser Felstechnik AG. It arrived at the site on 26 March 2002. The transfer wagon and auger components were installed on 26 and 27 March 2002 and had to be assembled together as a unit in the EB access tunnel (Figure 38). Evaluation of the access into the site with the auger after mounting it on the transfer wagon indicated that modifications to the emplacement equipment were needed in terms of changing the height, angle and length of the auger, as well as to the transfer wagon

wheel placement and height relative to the EB entryway tunnel height. These were done on site and finalized on 2 April 2002.

The processed Spanish Serrata bentonite was delivered to the site directly from the producer (Rettenmaier & Söhne AG). The shipment consisted of a total of about 47 tons in 63 big bags. It arrived at Mont Terri on 26 March 2002 in enclosed transport trucks and each big bag was well protected against physical damage and from moisture uptake. Each big bag had a double polyethylene liner and was tightly sealed on its bottom as well as top covers. In addition, the outside of both the bag and its own transport palette had been shrink wrapped with a tight and multi-layered plastic covering.

Figure 38: Auger and transfer wagon component assembly in EB entry tunnel: Transfer wagon (A) being moved under suspended Auger hopper (B) with auger boom (C) extending ~6 m forward for emplacement. Auger supported and suspended in the entryway (D)

The quality assurance aspects of the emplacement were based on mass balance calculations and consisted of determining the weight and water content of the GBM. The weighing was done in two steps. The first weighting of each of the big bags was performed at the producers facility prior to shipping. Their weighing station had a resolution of about +/- 1 kg. The second weighing of the big bags was done just as the bags were being transported from their temporary storage near the EB niche to the emplacement equipment. The weighing on site was done with a scale with a resolution of +/- 10 kg. In this manner there was an accurate record kept of the weight of the material as it was emplaced. The total weight of the 55 big bags containing the materials that were used for the emplacement was determined as 40765 kg (Rettenmaier) and 40650 kg (EB niche). The difference of 115 kg represents an error of less than 0,3 percent. The accuracy of the scale at Rettenmaier was better and therefore, the weight determined from their scales was used in the calculations.

Samples were taken and analyzed on-site for the water content of the GBM. The samples were taken from each big bag as it was emptied into the transfer wagon hopper. Several locations were used from around the hopper to reach the total sample volume in order to achieve as representative as possible a mixture of the entire materials in the bag. The weight of the samples and the big bags is estimated to be 3 - 4 kg per big bag for a total of 165 - 220 kg of mass not emplaced.

The water content of the samples was determined immediately after sampling. The average water content from 53 big bags (two samples were lost) was 4,17 percent with a minimum of 3,52 percent and a maximum of 4,81 percent. Also, 19 grain size analyses were performed. The results show a wide grading band, with the following average values:

	Size							
Average percent passing	10 mm	6,3 mm	5 mm	2 mm	1 mm	0,5 mm	0,25 mm	0,125 mm
	95	50	45	40	22	14	10	8

Then, it can be estimated that the average D_{50} of the GBM is about 6,3 mm; and the average D_{10} about 0,25 mm.

5.3.1 Emplacement pre-conditions

The volume to be filled had constraints and restricted movement that would result in obtaining less than optimized compaction due to the presence of instruments, cables and the saturation system (Figure 37). Within the retaining wall window, through which the auger had to move, there were only three possible "access" channels for the auger to enter over the test section length. These three locations were a) in the center above the canister between, b) to the left of and c) to the right of the uppermost two saturation tubes and the cabling that suspended the two next lateral saturation tubes.

The presence of the saturation tubing limited first, the amount of compaction in the upper part of the test section and second, the compaction from free falling of the GBM. There is a high force associated with the extrusion of the bentonite when the head of the auger is in the material. In the model runs during the trials, the auger head was left in the material as much as possible to achieve added compaction. In the case of the emplacement in the EB test section, such a high compaction was not able to be reached. The risk of rupture of the saturation tubing coming from the auger meant the time of auger head burial was kept at a minimum and thus the volume of material subjected to this higher degree of compaction was lower than planned. The second effect of the saturation tubing and its support cables and of selected instruments that penetrated into the open volume, was to create the potential of localized pockets (shadow zones) that could create additional void spaces and reduced compaction.

5.3.2 Emplacement actions

The emplacement activities began on 2 April 2002 and were completed on 5 April 2002.

On day one (2 April, 2002) a total of 15 big bags containing a mass of about 11,3 T were emplaced in 4 h. This activity was targeted in the rear of the EB test section so that the open space between the canister and the end wall, and the back corners continuing around to both sides of the canister, would be filled. There was no possibility of access to the rear of the test section to undertake anything other than the compaction resulting from the fall of the material from the auger.

On day two (3 April 2002), backfill activities continued with a total of 18 big bags containing a mass of about 13,4 T emplaced in 9 h. The target on this day was to complete the backfilling as high as possible

along and to the left hand side (LHS) of the canister. This involved moving the equipment so that the auger could enter to the left of the saturation tubing, to the extent possible, with the auger directly against the LHS of the retaining wall access window. During this time, the emplacement actions of the auger were also augmented by manual compaction, to the extent possible, of regions surrounding the tubing and close to the walls. This was undertaken to overcome the shadow effects that were observed and discussed above and to compensate to some degree for the reduced compaction arising from the presence of the instruments, cables and lines.

On day three (4 April 2002), backfill activities continued with a total of 16 big bags containing a mass of about 11,2 T emplaced in 10 h. The target on this day was to complete the backfilling as high as possible along and to the right hand side (RHS) of the canister. The filling on the RHS also involved manual compaction where possible. Further, in order to get fill beyond two instruments located on the LHS, material was deposited in the top near the rear and manually pushed from the top section laterally to fill that area. The auger could not penetrate beyond this point without damaging the instrumentation, so we elected to use a manual approach to backfill in this area. Furthermore, in the emplacement by gravity along the RHS, there was also spillage and migration of the slope as the granular material spread around the edges of the concrete bed so that the front of the test section between the canister and the retaining wall became partially filled.

On day four (5 April 2002), backfill activities were completed with a total of 5 big bags containing a mass of about 4,5 T emplaced in a period of about 8 h. The markedly lower emplacement rate was a result of the extra work related to sealing in the top section and at the entrance with the retaining wall window seal. Materials at the back and to the sides of the top section in the last 0,20 to 0,30 m of height were manually adjusted in certain areas in order to avoid damaging the saturation lines attached to the ceiling.

The total mass emplaced was about 40,2 T in an estimated available volume of about 28,4 m^3. The obtained dry density (ρ_d) of the GBM was 1,36 g/cm^3. This value is about 3% lower than had been achieved in the trials (about 1,40 g/cm^3). A higher density, similar to what was achieved in the model, would be expected a) without the presence of the physical obstructions of the artificial saturation tubing and its supporting materials and b) by allowing the auger head to remain buried in the materials to extrude as much of the granular material as possible under higher compaction.

Estimated parameter value ranges associated with grain density values of 2,58 and 2,70 g/cm^3, respectively, for the emplaced GBM are:

Void ratio	0,90 to 0,98
Porosity	47 to 50 percent
Degree of saturation	11 to 12 percent
Air volume	11,8 to 12,5 m^3

6 EXPERIMENTAL RESULTS

6.1 Water intake

The hydration of the buffer started on 6th May 2002. The water intake was faster than initially expected and it was stopped after some water stains appeared on the walls. A total of 6700 litres of Pearson's water were injected to the system in only two days during this first hydration phase.

The second phase of buffer hydration started on 11th September 2002. Several electrovalves were installed to allow the injection be automatic, at a maximum rate of 25 litres in ten minutes each day approximately. This phase continued for more than a year.

From the first week of September 2003, several problems were detected due to the higher injection pressure required to maintain the water injection. On the 22nd October 2003, a new continuous injection system was installed. In total 15165 litres of water has been injected until the end of October 2003. It should be pointed out that in the test section the estimated total air volume before the start of the water injection was about 12500 litres. A possible explanation for this discrepancy is that some water is flowing towards the rock mass and through the concrete plug. Also, it may be that the density of the interstitial water of the bentonite is greater than one.

6.2 Hydro-mechanical data

Data have been collected by means of the Data Acquisition System from the moment of installation, in May 2002. Some data were collected with data loggers from November 2001 to April 2002. The DAS has been continuously working for a period of 18 months.

6.2.1 Temperature

All the sensors include temperature probes, except the in-rock pore pressure ones.

There was a clear temperature increase after the starting of water injection, reaching a maximum peak of 28 ºC in one of the sections, due to the fast hydration of the buffer. In general, after that initial peak, the temperature remained at about 4 ºC above the recorded values in the beginning of data collection for a period of three months. After this time, temperature has progressively recovered the initial values.

6.2.2 Total pressure

In general, pressures show gradual increase from the starting of buffer hydration in May 2002. See Figure 39 for evolution of total pressure cells and Figure 9 for position in section E.

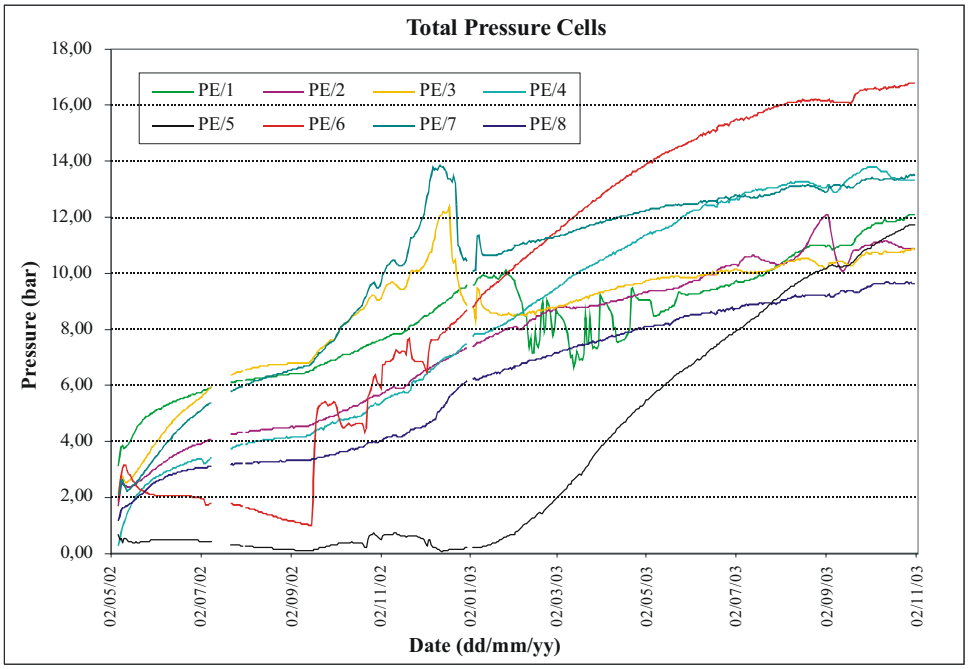

Figure 39: Section E, evolution of total pressure cells

6.2.3 Relative humidity

All sensors installed into the rock mass reached saturation after one year of hydration. See Figure 40 (Data available since November 2001 collected by data loggers and DAS). Initial relative humidity values higher than 100% recorded at some sensors might be due to water condensation after their installation.

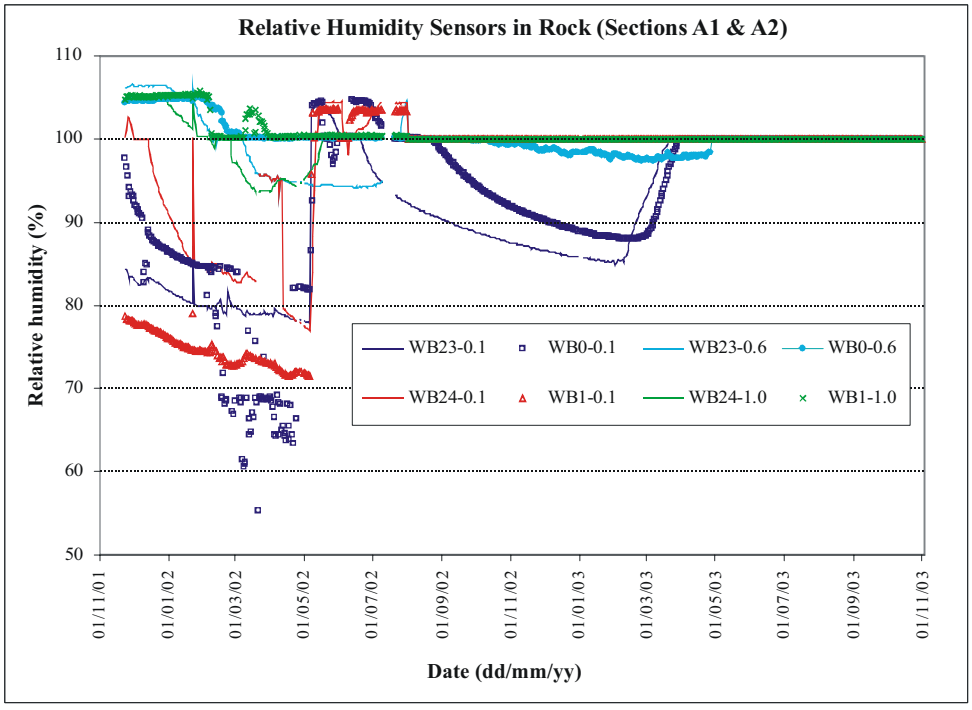

Figure 40: Sections A1 and A2, evolution of relative humidity in rock

The general response of the hygrometers installed in the buffer was a gradual increase of relative humidity after the start of the 2nd injection phase in September 2002, with different gradients of humidity

change. All sensors but one, located in the granular backfill of section B1, reached saturation after the first year of hydration. See Figure 41 (Data available since May 2002, collected by DAS) and Figure 10 for the location of the sensors.

6.2.4 Displacements

There are two types of extensometers installed, to measure the movements of the rock walls (see Figure 9) and to measure the canister displacement (see Figure 8).

The extensometers located at both sides of the niche have registered a small horizontal closing of the drift. On the other hand, the extensometers installed on the roof registered an upwards movement of the gallery but from May 2003, this tendency reversed.

The canister moved upwards few millimetres in the start of data collection and seems to have remained in the same position the rest of the time.

6.2.5 Rock pore pressures

The vertical piezometers (installed in boreholes BEB-3 and BEB-22, see Figure 10 for location) increased their pressure values up to about 12 bar. The pressure increases with depth (see Figure 43).

The inclined piezometers (installed in boreholes BEB-2 and BEB-21, see Figure 10 for location) showed a similar behaviour than the vertical ones, but those at deeper positions reached lower pressure values.

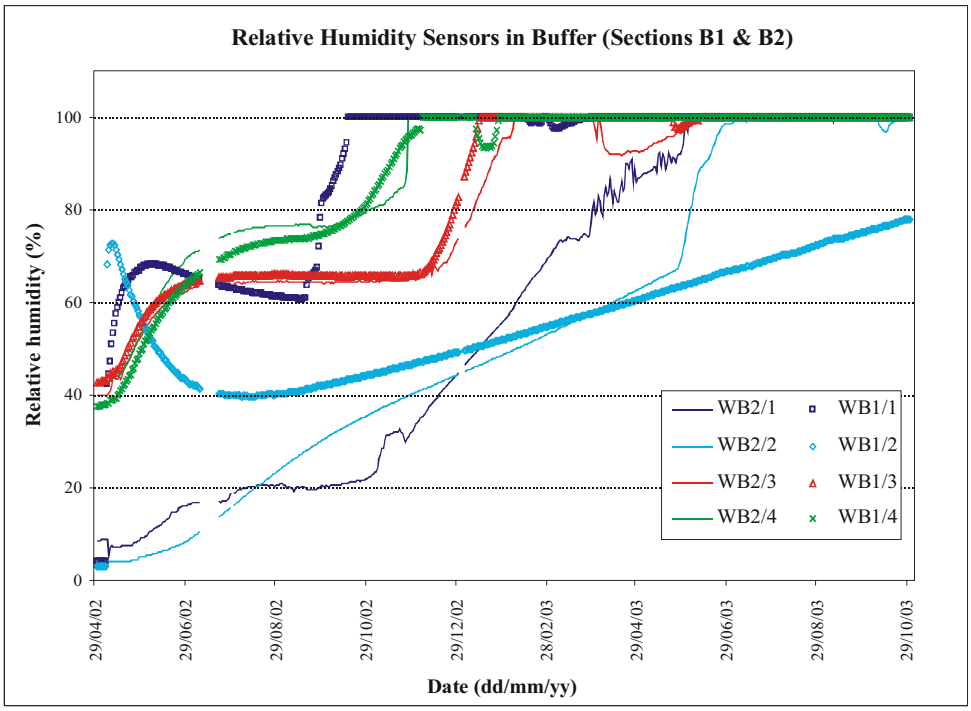

Figure 41: Sections B1 and B2, evolution of relative humidity in buffer

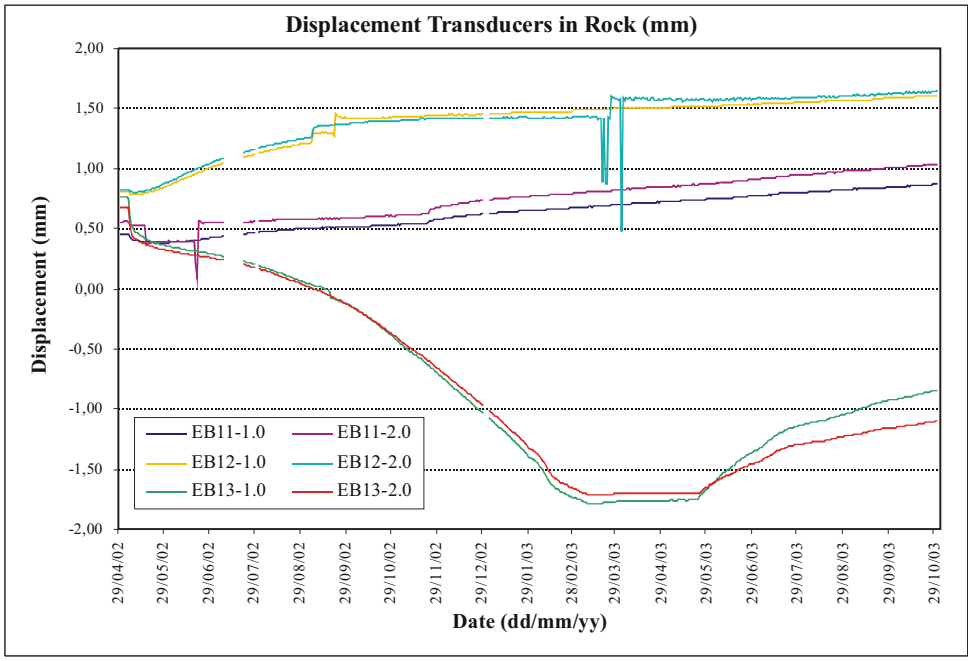

Figure 42: Evolution of rock displacement sensors

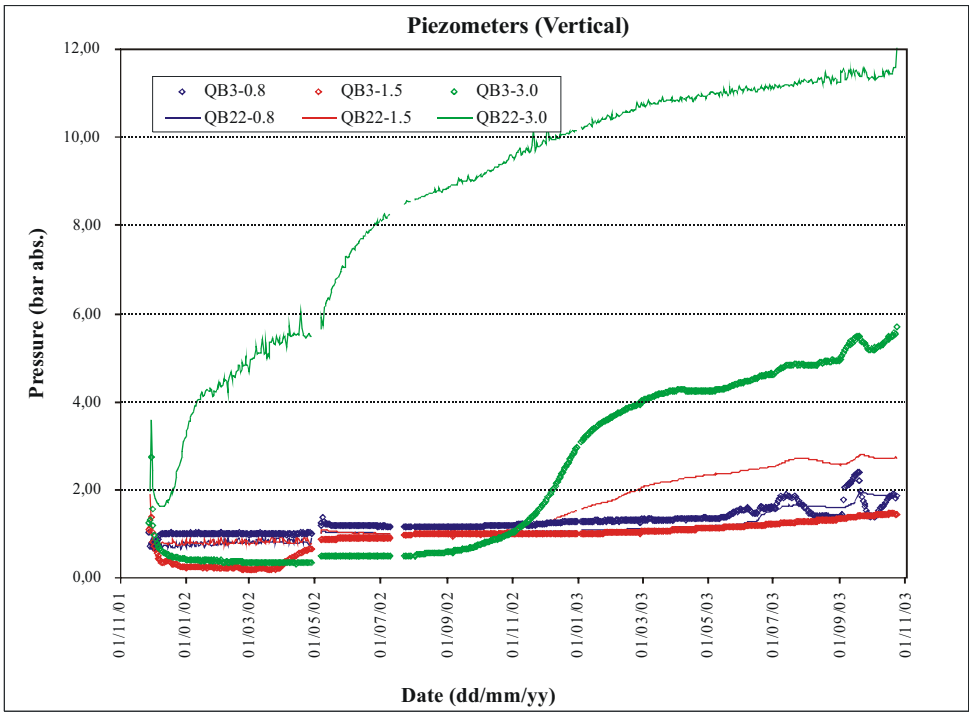

Figure 43: Evolution of rock pore pressures

6.3 Geophysical data

Monitoring of seismic velocities was performed using four parallel boreholes drilled 45° upward into the tunnel wall (Figure 44). The four holes were drilled in the central part of the tunnel with a distance of about 1 m to each other at the corners of a square. The holes were instrumented with piezo-electric

transducers at depths of 8, 38, 68, 138 and 208 cm. With this instrumentation the crosshole seismic responses between these holes were determined at the according depths. In addition four transducers were installed in the backfill, one transducer 20 cm in front of each borehole.

Since 30th of April 2002 the seismograms between all transducers were recorded automatically once a day until 26th of November 2003. The data acquisition system partially failed for 45 days between day 451 and 493 (August 2003). Figure 45 shows the obtained seismograms between the four transducers placed in the backfill. Only every fifth trace is plotted. Initially, after backfilling and beginning of saturation no response was observed between these transducers. A first indication of increasing amplitudes and decreasing travel times was identified after 50 days between the two receivers closer to the plug shown in the upper left seismogram plot in Figure 45 (Direction of transmission 1; see Figure 44 and small insertion in Figure 45). It can be seen that the amplitudes increase and travel times decrease further during the following 400 days till end of June 2003. Then, after day 450 the amplitudes and travel times reach an almost constant level. Between the two upper transducers (Direction of transmission 2) first response was observed after 100 days during beginning of August 2002 (upper right seismogram plot in Figure 45). Amplitudes increased and travel times decreased during the following 300 days and both stayed about constant for the rest of the observational time. The responses observed in these two directions are small compared two the results of laboratory tests. This indicates that the backfill in this area seems not completely saturated. There are only very late and weak responses between the two lower receivers and the two receivers further in the back of the tunnel (Direction 3 and 4) as can be seen from the two lower seismogram plots in Figure 45. Very weak responses after about 300 days (End of February 2003) demonstrate that the instruments are operating. Obviously the pellets in the vicinity of the lower back sensor are only weakly saturated.

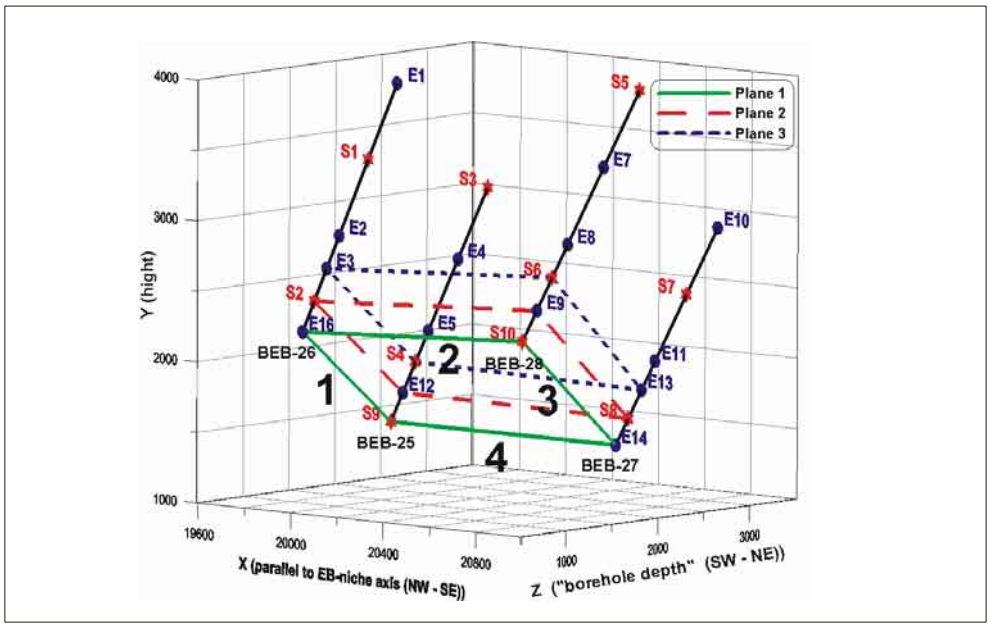

Figure 44: Layout of the seismic monitoring array. Seismic receivers are numbered in blue, seismic sources are numbered in red. Plane 1 is situated in the backfill. Plane 2 and 3 in the surrounding rock

Figure 46 summarizes the seismogram plots for the four main directions of transmissions namely for the backfill (Plane 1) and at four depths in the surrounding rock (Plane 2 to 5). Results for the backfill correspond to Figure 45. The four planes in the rock show two groups of similar results: In plane 2 and 3 in all directions initially weak amplitudes and large travel times are observed. For these planes the seismograms for some directions of transmission changed significantly during the experiment. Plane 4 and 5 show strong signals and small travel times from the beginning of the measurements for all directions. The travel times in these planes are as expected from intact rock and did not change during the

time of observation. Plane 4 and 5 thus can be assumed to lay in the intact rock and are not affected from the experiment. This interpretation is in accordance with the initial geophysical characterisation indicating an EDZ of about 65 cm in this area.

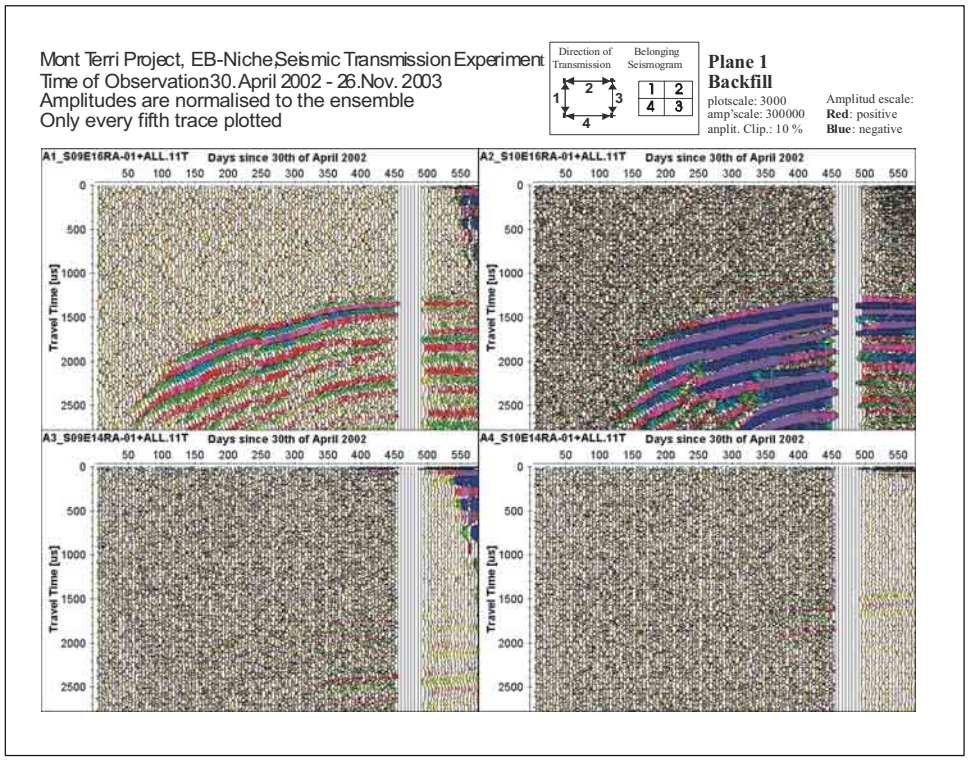

Figure 45: Seismogram plots for plane 1 (in the backfill) for the four main transmission directions

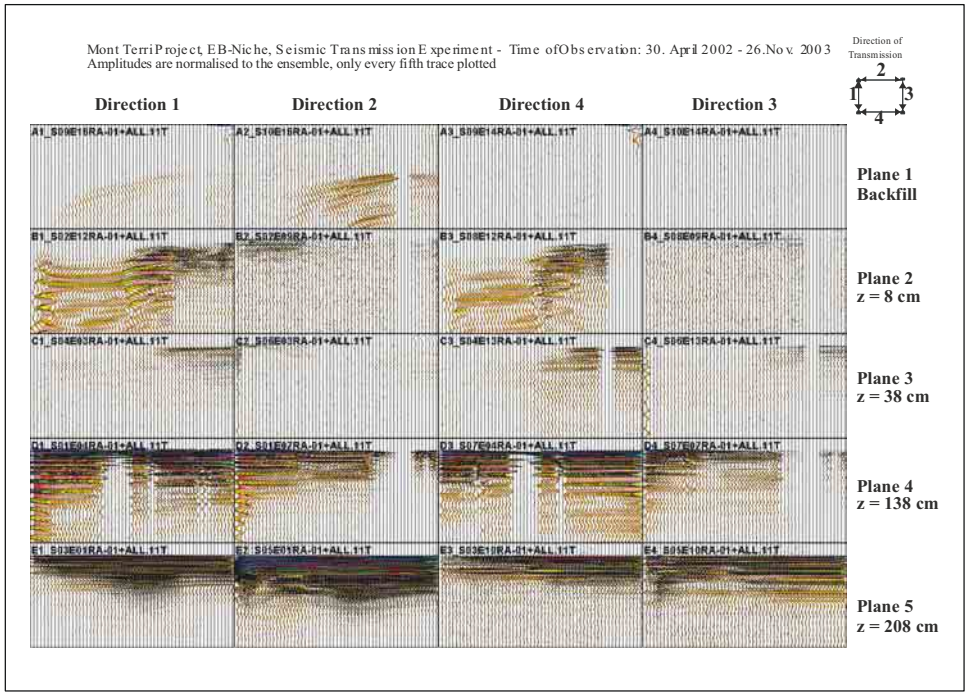

Figure 46: Seismogram plots for planes 1 to 5 for the four main transmission directions. Plane 1 is situated in the backfill, plane 2 and 3 in the EDZ, plane 4 and 5 in the intact rock

For plane 2 strong amplitude increase and travel time decrease is observed only some days after initiation of saturation in the directions 1 and 4. After 20 days the seismogram characteristics do not change any more for about 200 days. Then after 250 days (beginning of January 2003) an additional amplitude increase and travel time decrease was observed. The travel times after 350 days reach the values close to those for intact rock. Much weaker or none responses are observed for the directions 2 and 3.

For plane 3 the changes are even less than in plane 2. Again the directions 1 and 4 show the strongest effects. However the amplitude increase is much smaller as in plane 2 and can only clearly be identified after 270 days (direction 4) or 350 days (direction 1and 3). Despite of the weak amplitude response the travel times for the directions 1, 3 and 4 are close to the travel times of intact rock.

The sensors in the boreholes were also used to monitor the acoustic emission activity in this area. The seismic measurements showed a very strong attenuation of high frequency components. According to this observation the extension of the monitoring area is very poor. On the other hand the frequency of crack formation is very low. Both facts led to a small rate of acoustic emission events. During an observation interval of 13 months only 100 events could be stored and only 19 events could be localised three dimensionally. The localised acoustic emissions are located between 10 and 90 cm from the tunnel wall (Figure 47) and close to the upper left borehole. The depth corresponds to the extent of the EDZ. Due to high location uncertainty it was not possible to find structures indicating larger fractures.

During the second half of 2003 increased activities in the Mont Terri Laboratory induced acoustic emission activity not created by the experiment. The data processing and interpretation for this period is extremely difficult and still going on.

The geoelectrical measurements were conducted at two horseshoe-shaped profiles “Circular Profile 1” and “Circular Profile 2”, each consisting of 45 electrodes, which are fixed 21 cm apart. Additionally, a horizontal profile was mounted along the tunnel wall at a height of 1 m above the ground. This profile is 5.5 m long and also consists of 45 electrodes in a separation of 12.5 cm (Figure 48).

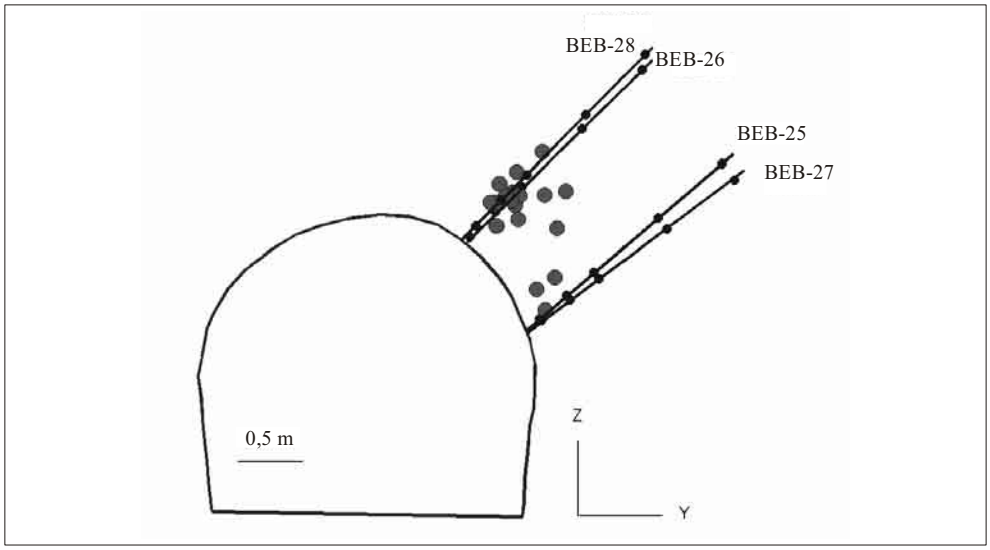

Figure 47: Localised acoustic emissions. View from rear of the tunnel towards the concrete plug

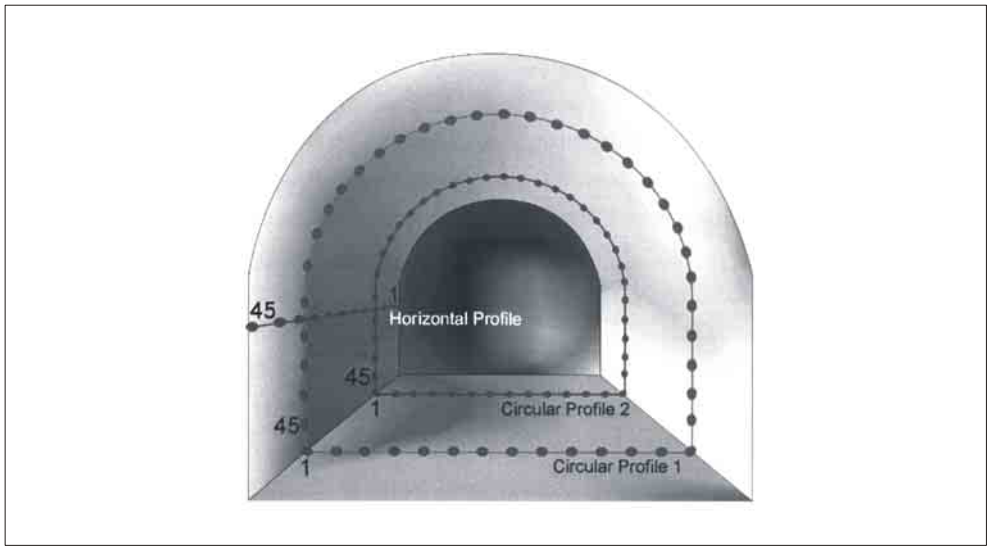

Figure 48: Installation of the geoelectrical profiles

The inversion results for the horizontal profile are pictured in Figure 49. The symmetrical distribution of the resistivity is caused by the one-dimensional layout of the electrode array within in a three-dimensional environment. Both figures show very low resistivity values near the electrode array and slightly increased values at higher distances. Additionally, a high-resistive anomaly appears on the left part of the profile that faces to the concrete plug. A striking difference between both inversion results is an anomaly in the 2002-measurements from 3 – 5 m in the horizontal length and about 0.5 – 1.5 m in the radial distance from the profile. The anomaly disappeared entirely in the 2003-measurements. The initial anomaly was also identified by the measurements for initial characterization of the EDZ.

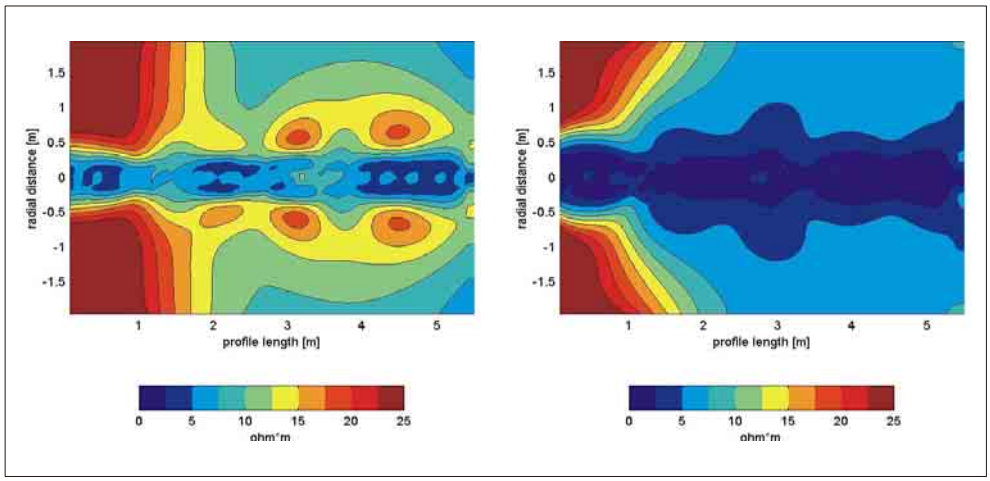

Figure 49: Display of the horizontal profile inversion results (Left: Nov 2002; Right: November 2003). The backward part of the tunnel is on the right side, the concrete plug on the left

The low resistivity in the profile's vicinity might be explained by a higher porosity in this area. This would result in a higher water proportion and therefore in lower resistivity. The increasing resistivity with

increasing distance from the profile does not necessarily indicate a lower porosity or any other inhomogeneities within the backfill material. It is also possible, that this effect is caused by inhomogeneous water content within the Opalinus Clay.

The high-resistive anomaly on the very left is probably a result of the concrete plug. Concrete is a very resistive material and therefore the plug reduces the space for the current to propagate.

The inverted data for the circular profile 1 are displayed in Figure 50. The measurements in 2002 show three major high-resistive anomalies with resistivities greater than 100 Ωm and a low-resistivity background with resistivities less than 10 Ωm. The anomalies are located at levels of approximately –1 m corresponding to the concrete floor, at 0 m corresponding to the installed canister and at about 1,4 m. The anomaly at 1.4 m could either be evoked by the EDZ or by an incomplete saturation in the upper part of the backfilling, or by a mixture of both. Another large anomaly appearing in the upper left corner can be assumed to be a "side-block-effect" deriving from the inversion process and must not be seen as a geological structure.

The inversion-results from the 2003-measurements show only two large anomalies, corresponding to the concrete floor and to the canister. This second anomaly fits into the actual shape of the canister almost perfectly. However, a small anomaly with maximum values of approximately 50 Ωm springs up left of it. The uppermost anomaly at a height of 1.4 m declined to a large extent, only a small anomaly with maximum values of 30 Ωm remains. However, another anomaly appears on the left side of the canister, but this one can be ascribed to the canister. The inversion results of the circular profile 1 show the canister as an electrically very high-resistive body, because the lacquer coat that surrounds the canister prevents the current flow from entering the canister's steel mantle. The upper part of the tunnel's backfilling is clearly different from the surrounding clay; the lower part however shows hardly any resistivity contrast. There is no contrast between the bentonite blocks from the canister's platform and the surrounding bentonite pellets.

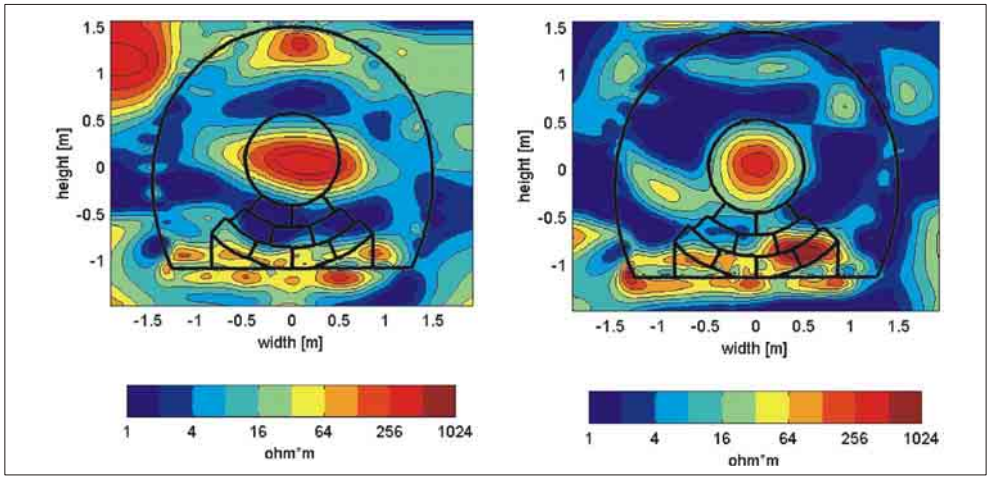

Figure 50: Display of circular profile 1 inversion results (DC-data. Left: November 2002; right: November 2003). The results are displayed in logarithmic scale

6.4 Hydro-testing results

The hydrogeological characterisation has been continued after the beginning of the hydration with three additional measurements in September 2002, February 2003 and October 2003. Figure 51 shows the obtained hydraulic conductivity for all five campaigns as a function of interval depth. In all campaigns the highest hydraulic conductivity was observed at a depth of about 60 cm. For two high hydraulic conductivity at a depth of 23 cm (February 03 and October 03) the flow rate response indicates a flow boundary.

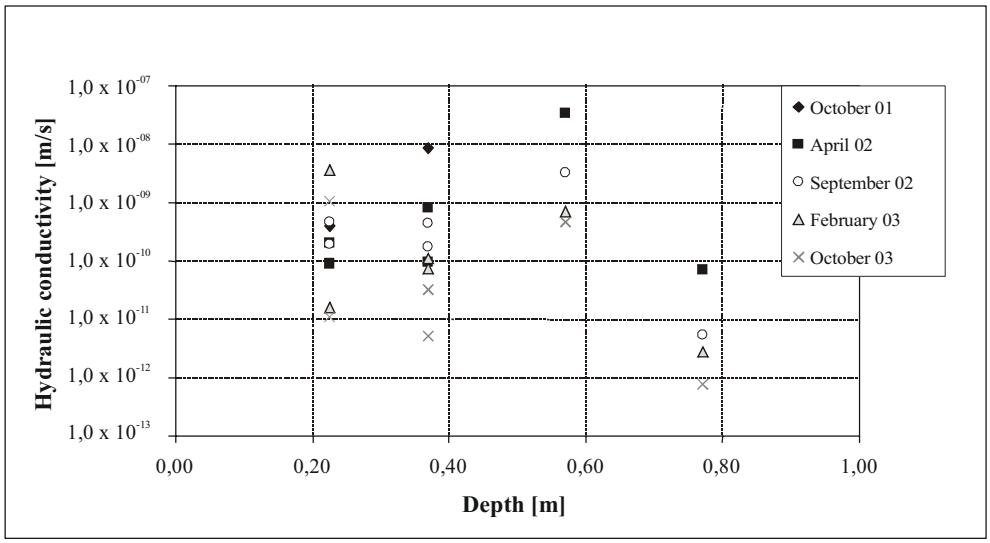

Figure 51: Hydraulic conductivity measured during the five campaigns as a function of depth from the tunnel wall. Results are only shown for constant head tests

During the time of observation the hydraulic conductivity decrease generally by two orders of magnitude (Figure 52). The exceptions for a depth of 23 cm have been discussed before. There is no change in the general trend between the results obtained before the beginning of hydration (October 2001 and April 2002) and results obtained afterwards. Thus it is not clear whether the observed decrease is due to the hydration of the backfill and EDZ or just due to the saturation around the borehole due to the test itself. In addition for several boreholes the response shows that even after 18 months of artificial saturation of the EB-site, not all boreholes are saturated. This may be due to a connection between the boreholes and the atmospheric boundary which prevent the complete saturation of the EDZ fractures.

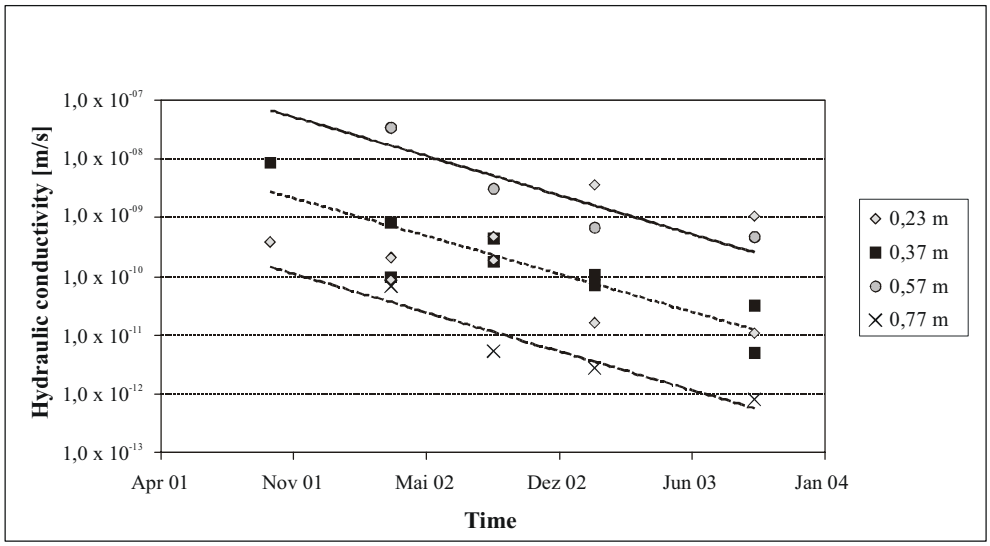

Figure 52: Hydraulic conductivity measured during the two campaigns as a function of time. Results are only shown for constant head tests

7 INTERPRETATION AND MODELLING OF EXPERIMENTAL RESULTS

The two dimensional, plane strain, Finite Element model developed is represented in Figure 53. CODE_BRIGHT was the computational tool used in all cases. Once the initial and boundary conditions were assigned, the tunnel excavation and test installation was simulated.

For the simulation constitutive model developed for argillaceous rock is used for the simulation. The model is able to integrate important features such as elastic degradation along loading and drying paths, brittle behaviour during shearing and permeability increase due to damage.

Parameter values used in case of bentonite blocks were derived from FEBEX data and they are reported in FEBEX Final Report 1/2000. In the case of the GBM, parameter values were adopted based on the information coming from the laboratory test program performed by UPC. According to these results some general patterns of the hydro-mechanical behaviour of the GBM can be remarked. The most important aspects of the observed behaviour can be summarized as follows:

- GBM has shown a remarkable bi- modal structure; and then the hydraulic and mechanical response presents some specific patterns, which makes the pellet mixture different from "regular" compacted expansive soils.
- The hydration phase of the GBM can be divided in two parts. In the first stage, the hydraulic properties of the macrostructural level will control the water inflow rates (very high water permeability values are associated with this structural level). After this initial period the expanding deforming pellets block the incoming water, controlling the hydration kinematics. In Figure 54 a simplified view of the described phenomena is presented.
- The mechanical response of the material is also explained by the bi-modal structure of the pellet mix.

Parameter values for GBM were selected according to the following ideas:

- It behaves as an almost granular material during the first part of the hydration phase.
- Model parameters were defined considering the general patterns of the swelling behaviour of the material. This behaviour is controlled by the overall dry density.
- Two permeability values were adopted. During the first part of the hydration phase, where very high inflow rates were registered, a very high permeability value was assumed. After this initial period, material permeability was progressively decreased to the saturated value.
- Special care was placed in modelling the fundamental behaviour of the material during the second stage of the hydration phase regardless of the initial period where the fast flooding of the material occurs.
- Comparison of model calculations and "in situ" measurements

Figure 55 shows the calculated water pressure field at the end of the ventilation period (95 days). It is strongly dependent on the relative humidity value assumed inside the tunnel. According to the in situ measurements, the relative humidity values registered in sensors emplaced at a distance of 0,1m of tunnel wall were about RH(%) = 80. No major differences were observed between values obtained in sensors emplaced at distances of 0,6 and 1,0 m of tunnel wall where values of around RH(%)=95 were registered. Based on these results the relative humidity value assumed inside the tunnel during the 95 days of natural ventilation seems to be greater than the "in situ" value. Despite this discrepancy no major difference appears to be between model predictions and observed behaviour.

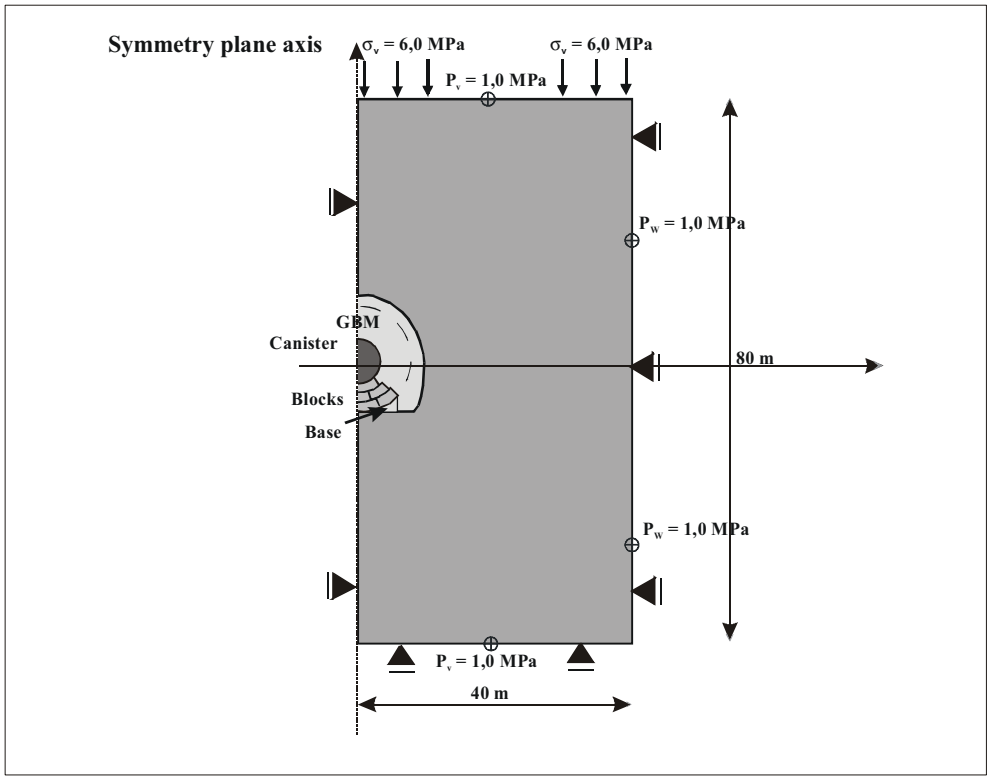

Figure 53: Model geometry and boundary conditions

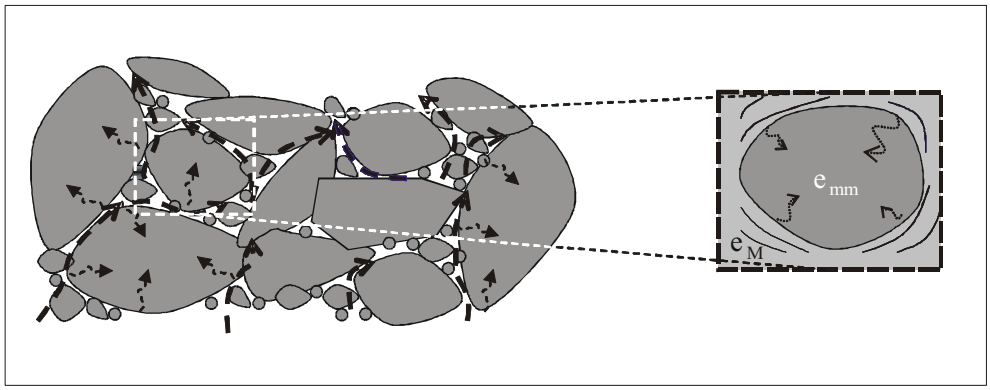

Figure 54: Synthetic view of the hydration process. Water flows, if boundary conditions allow it, through the network of macropores. Pellets hydrate from the water existing in open voids

The analysis of the EDZ evolution is presented in terms of the damage multiplier of the model. This parameter has a null value when the rock is in an undamaged state and a positive value when the rock is damaged. Figure 55 shows the geometry of the EB niche and the calculated contours of equal damage multiplier. Damage is proportional to the value of this parameter. At end of the excavation, the calculated damage zone reaches a maximum thickness of 0,30 m at the sidewall and 0,60 m on the niche crown (Figure 56). This is in complete accordance with the measurements reported by BGR. Measured values by means of geophysical methods range between 0,10 m to 0,15 m on the sidewall and 0,50 to 0,75 m on the roof. Computed damage is larger at the tunnel roof than at the tunnel sidewalls, a result related to the shape of the tunnel cross section and to the initial state of stress.

A comparison between the observed and computed suction evolution, for the WB13 and WB14 sensors (section B1), is presented in Figure 57. The evolution of the injected water volume is represented in the plot together with the evolution of suctions, in order to relate the suction response with the different wetting episodes. After the first hydration phase, where a volume of about 6700 litres of water was injected in a two day period, the suction started to decrease.

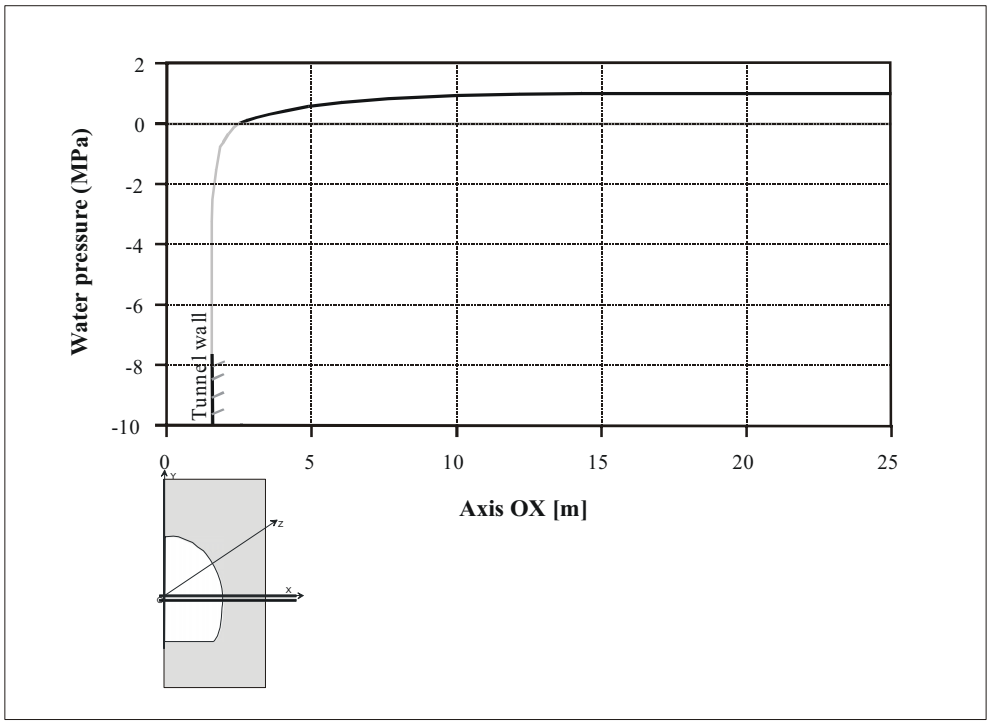

Figure 55: Water pressure field along axis OX after 95 days of tunnel opening

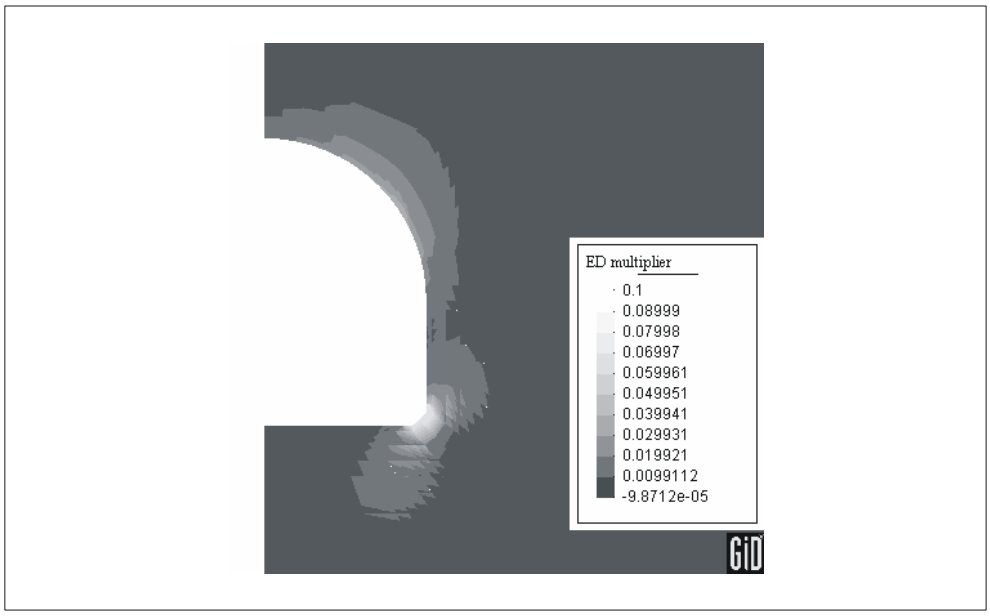

Figure 56: Representation of the EDZ 95 days after tunnel excavation. Contour for zones with equal damage multiplier values are represented

In other sensors located in section B1 (sensors WB11 and WB12) the suction decrease in a fast way. In section B2 (sensors WB21 and WB22) a slower rate in the suction decreasing evolution was observed. Significant discrepancies are observed between the real and computed results during the first hydration phase. Calculated results predict a suction decrease to a value of around 3 MPa during this period. Discrepancies could be explained because of the complex and heterogeneous evolution of permeability of the pellet mixture as it becomes wetted.

Measured and computed values for the stresses in the pellet buffer material are presented in Figure 58. Good agreement is found between computed and predicted stress evolution, specially for the vertical stress sensors (PE1 and PE2). Swelling pressure evolution observed in sensors PE1, PE3 and PE7 shows some particular drops that could be associated to the general collapse of the granular arrangements. These observed effects could not be reproduced in the numerical simulations despite the constitutive model used for the bentonite pellets is specially suitable to capture these type of phenomena.

Computed results for the swelling pressure of bentonite blocks reproduce satisfactorily actual measurements. No drops in the swelling pressure evolution are observed in the bentonite blocks due to its high dry density.

A further insight into the wetting and swelling processes taking place in the buffer is provided by the stress paths actually followed by representative points. A plot of this kind, showing the progressive development of swelling pressure as suction decays is given in Figure 59. In some points (sensors close to the canister), a marked pressure peak, probably associated with a faster wetting, is recorded. In points closer to the rock a continuous increase in swelling pressure is recorded.

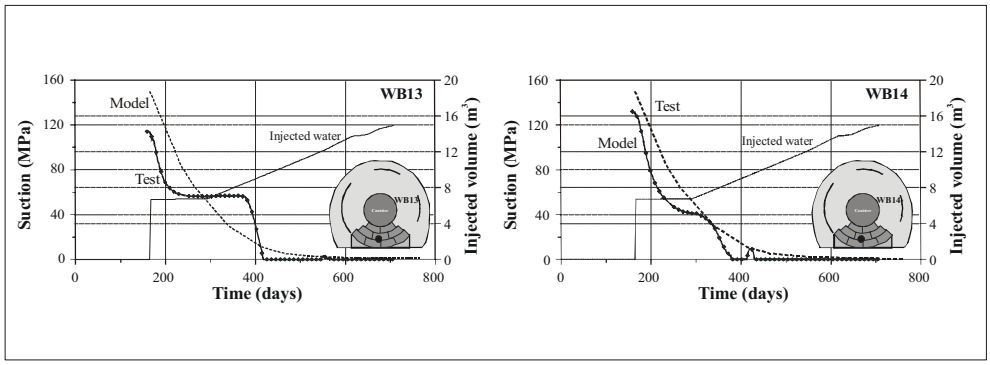

Figure 57: Evolution of observed and computed suction evolution in the bentonite blocks buffer material in section B1

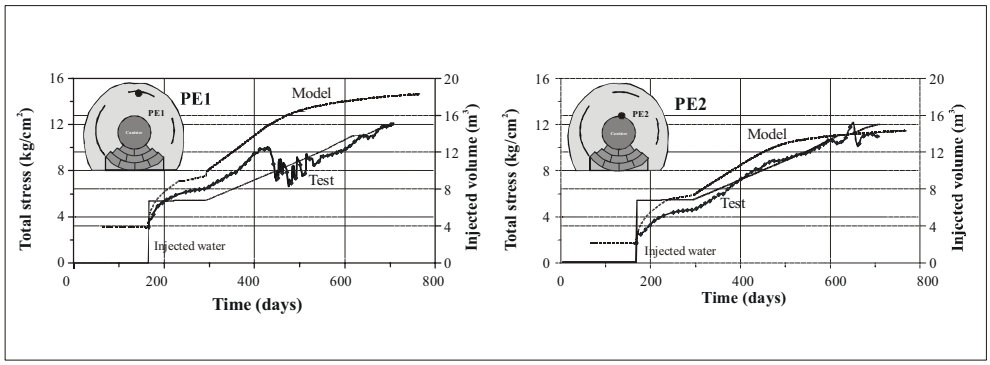

Figure 58: Evolution of the observed and computed swelling pressure for the bentonite pellets in sensors PE1 and PE2

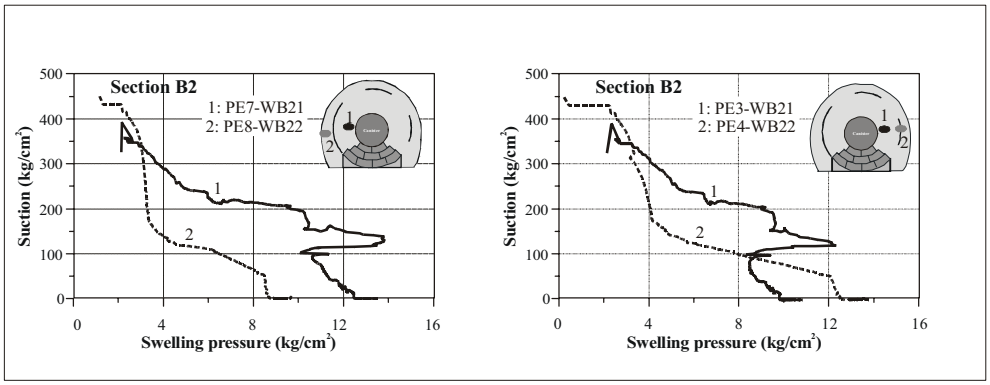

Figure 59: Evolution of the swelling pressure and suction in the pellet buffer material

7.1 Conclusions

A good estimation of the thickness of the rock EDZ is derived from calculations. A reasonably good agreement was found for suction evolution ad swelling pressure development. However, field measurements of the buffer relative humidity (suction) indicate a marked heterogeneous behaviour which cannot be reproduced by the model. The heterogeneous response of the buffer is explained by the irregular hydration of the buffer which is a consequence of the emplacement conditions and the nature of the evolving permeability of the GBM.

8 ASSESSMENT OF RESULTS AND CONCLUSIONS

The EB experiment has proved that fully automated production of a Granular Bentonite Material (GBM) is possible and large quantities can be produced in due time in the required quality. Only minor modifications of existing production lines in industry for other applications were necessary to achieve this result.

In the EB test section, a dry density of 1,36 g/cm^3 of the emplaced GBM has been obtained. With this value it is estimated that the hydraulic conductivity of this material is lower than 5×10^{-12} m/s and the swelling pressure is about 1,3 MPa.

Even though the EB test section conditions are now not considered as representative of a true demonstration, it is deemed that the model emplacement testing results (dry density of about 1,40 g/cm^3) serve well to demonstrate the achievable densities expected in the real world setting. The artificial hydration system removes the reality of this as a true demonstration site but without it, the work could not be conducted in a reasonable experimental time period, so that the suggested technical approach seems a good compromise.

The combination of the hydro-mechanical data obtained in this project and the knowledge gained from other projects under a variety of conditions (natural/artificial saturation) have brought very useful information for assessing the performance of this barrier system. The backfilling methodology developed in the project is a promising solution, which is certainly worth considering in the future although some improvements could be made in order to increase the dry density of the GBM and to get a more homogeneous buffer.

On the other hand, geoelectric and seismic measurements have proven to be a good complement of the hydraulic testing methodology of the EDZ evolution during saturation. The investigations on the time dependent evolution of the EDZ strongly support the hypothesis of EDZ self-sealing in Opalinus Clay, and is thus an excellent completion of the work done in the SELFRAC experiment under contract with the EC, as well.

Mathematical model calculations have been compared with field measurements. A good estimation of the rock EDZ is derived from calculations. Buffer response was compared with measurements at the position of the monitoring points. A reasonably good agreement was found for suction evolution and swelling pressure development. However, field measurements indicate a marked heterogeneous behaviour which cannot be reproduced by the model. The heterogeneous transient response of the buffer is explained by the irregular hydration of the buffer which is a consequence of the emplacement conditions and the nature of the evolving permeability of the GBM.

From December 2003 on, the EB experiment is in a latent monitoring phase and close to a full saturation situation, that is the time when the buffer is " fully operative " and acting on the rock. After this phase, and in order to check the performance of the buffer, the interface buffer/host rock and the influence of the saturated buffer on the EDZ state, dismantling of the test is recommended.

9 REFERENCES

9.1 EB Project internal deliverables

D01. AITEMIN; Engineered Barrier Emplacement Experiment in Opalinus Clay. "EB" Experiment. (Test Plan); July 2001

D03c. NAGRA; Granular Material Backfill Product Documentation; August 2003

D04. NAGRA; Granular Material Backfill Emplacement Methods Evaluation; September 2003

D10. BGR; Report on EDZ geophysical characterisation; July 2002

D11. BGR; Report on hydrogeological characterisation of EDZ; January 2004

D12. NAGRA; Granular Material Backfill QA Report with Emplacement Description; August 2003

D13. CIMNE; EB project. Scoping calculations; November 2001

D15-2. CIMNE; Reports on modelling and interpretation of results; November 2004

D16a-1. AITEMIN; Sensors data report No. 1; November 2002

D16a-2. AITEMIN; Sensors data report No. 2; December 2002

D16a-3. AITEMIN; Sensors data report No. 3; March 2003

D16a-4. AITEMIN; Sensors data report No. 4; June 2003

D16a-5. AITEMIN; Sensors data report No. 5; January 2004

D16b-1&2. BGR; Geophysical characterization of the EDZ 1&2; June 2003

D16b-3. BGR; Geophysical characterization of the EDZ 3; Included in D16b-4

D16b-4. BGR; Geophysical characterization of the EDZ 4; September 2004

D16b-5. BGR; Geophysical characterization of the EDZ 5; September 2004

D18-2. BGR; EDZ tests reports; January 2004

9.2 Other references

ENRESA (2000): FEBEX Project. Full-scale engineered barriers experiment for a deep geological repository for high level radioactive waste in crystalline host rock. Final Report. Publicación Técnica ENRESA 1/2000. 354 pp. Madrid.

C. Hoffmann, E.E. Alonso and E. Romero (2003). "Fabric changes of a pellet-based bentonite buffer and their effects on mechanical behaviour". Proc. International Conference on Coupled THMC Processes in

Geo-systems: Fundamentals, modelling experiments and applications (GEOPROC 03). Stockholm (Sweden) 1: 332-340.

J. Vaunat, E.E. Alonso and A. Gens. "A constitutive model for argillite: description and application to a mudstone". Internal report, Department of Geotechnical Engineering and Geosciences, Technical Uneversity of Catalonia (UPC).

J.J. Muñoz, E.E. Alonso and J. Vaunat (2003). "Development of damaged zones in the vicinity of the barrier-rock interface". Proc. European Commission CLUSTER Conference. Luxembourg (Luxembourg): 126-133.

J.L. Fuentes-Cantillana, J.L. García-Siñeriz (1998). FEBEX. Final design and Installation of the “in situ” test at Grimsel. Enresa Technical Report 12/98. Madrid.

Olivella, S., Carrera, J., Gens, A. & Alonso, E.E. (1996) Numerical formulation for a simulator (CODE_BRIGHT) for the coupled analysis of saline media. Engineering Computations, 13, 87-112.

APPENDIX

CONTACT DETAILS CONCERNING FOLLOW-UP OF THE EB PROJECT

Company	Contact person	Address
Empresa Nacional de Residuos Radiactivos, S.A. (ENRESA)	Juan Carlos Mayor	Research and Technology Division C/Emilio Vargas, 7 28043 Madrid Spain www.enresa.es
Asociación para la Investigación y Desarrollo Industrial de los Recursos Naturales (AITEMIN)	José Luis Fuentes-Cantillana	AITEMIN Alenza, 1 28003 Madrid Spain www.aitemin.es
Centre Internacional de Mètodes Numerics en Enginyeria (CIMNE)	Eduardo Alonso	Gran Capitán, s/n Edificio C1 Campus Norte 08034 Barcelona Spain www.cimne.upc.es
Bundesanstalt für Geowissenchaften und Rohstoffe (BGR)	Hans-Joachim Alheid	PO Box 510153 Stilleweg,2 3065 Hannover Germany www.bgr.de
Nationale Genossenschaft für die Lagerung radioaktive Abfälle (NAGRA)	Peter Blümling	Hardstrasse 73 5430 Wettingen Switzerland www.nagra.ch